ETH zürich

Soft Robotics Laboratory

Master's Thesis Report

Electrostatic Zipping Actuators With A Double-Helical Structure

Yu (Antares) Zhang

October 2023

Supervision

Dr. Ronan Hinchet
Prof. Dr. Robert Katzschmann

Abstract

Artificial muscles are key for creating soft and bio-mimetic robots. Despite substantial advances, current actuator technologies are still limited in their form factor and struggle to achieve high power and energy density while being efficient. This thesis focuses on a new actuator design that could potentially improve on those key metrics. We present an electrostatic zipping actuator with a double-helical structure. The thesis reports the inspiration, design, fabrication, testing, and evaluation of this electrostatic zipping actuator with double-helical electrodes. The topics of material selection, fabrication, insulation, and testing of various actuator prototypes are discussed. The challenges faced in the development process are described, and potential solutions for future research are discussed. The evaluation results are documented and compared with the project's initial goals. After overcoming various challenges in the design, fabrication, insulation, and testing of the actuators, the latest prototype was able to achieve active contraction and generate useful work from electrostatics. With limited time and resources, the recorded actuator performance did not reach the initial goal of surpassing the state-of-the-art actuators with 30% strain at 5N of contraction force but had the potential to when discussed and calculated in detail. Finally, potential pathways for future improvements are described. This report intends to provide guidelines for future researchers to continue the development of this promising actuator concept and eventually integrate such actuators into robotic applications. After the eventual optimization of this actuator concept, versatile bio-mimetic robots with significantly improved efficiency and reduced complexity can be built and bring humanity into the next era of human-robot interactions.

Contents

1 Introduction

The emerging field of soft robotics (Yasa et al., 2023) has attracted substantial interest from the scientific research community in the past decade (Laschi et al., 2016), (Hawkes et al., 2021). Unlike conventional robots with rigid links, soft robots utilize flexible and/or elastic components. The intrinsic "softness" of such robots allows for the development of bio-mimetic designs (Katzschmann et al., 2018; Li et al., 2021) with built-in compliance, which leads to safer interactions with humanity and nature. Those features play an important role in the ultimate acceptance and integration (Laschi et al., 2016) of robotic technologies into a wider audience.

1.1 Need for a New Generation of Actuators

For a robot to successfully perform its tasks, it is important to drive the robot with powerful, compliant, efficient, cost-effective, and resilient actuators. Conventional robotic actuation technologies generally involve electromagnetic motors (Hutter et al., 2016; Zhu et al., 2019) that are well-understood and easy to integrate. However, the rigid nature of such actuators forbids them from being integrated into soft robots. Another limitation of electromagnetic motors is the electric current required to hold their positions under load. This limitation makes them inefficient in many bio-mimetic tasks such as standing, squatting, and cargo-carrying.

This lack of suitable actuators has sparked research efforts into various actuation technologies and their applications in a soft robotic setting (Garrad et al., 2022; Helps et al., 2022; Kellaris et al., 2021; Li et al., 2021; Sîrbu et al., 2021; Wang et al., 2020). Following this trend, this thesis investigates the design, fabrication, and testing of a new actuator concept. First, a state-of-the-art review of soft actuator designs is given, and the limitations of each design are discussed. The limitations of current designs not only motivate the thesis but also lay out the requirements and goals for the resulting actuator prototype. Then, the methodologies regarding design, fabrication, and testing are described in detail. Finally, the project results and potential future work are discussed.

1.2 State-of-the-art in Actuators

In recent years, many types of soft actuator technology have been explored in the search for an ideal solution in soft robotic applications, and the current goal is to develop a soft actuator comparable to natural muscles.

Initially, pneumatically powered soft elastomer actuators (Marchese et al., 2015) were studied. Those pneumatic actuators typically involved shaping an elastomer (commonly silicone elastomer) into air-tight chambers with variable geometries and external constraints. By varying such design parameters, actuators with different actuation patterns can be designed and customized for desired tasks (Marchese et al., 2015). The issue with pneumatic actuation is the necessity for a pressure source usually composed of reservoirs, tubes, valves, and pumps powered by electromagnetic motors. This limits most application scenarios to tethered systems.

Another direction of research focused on electrostatic actuators. Unlike electromagnetic actuators, those actuators rely on electrostatic forces to generate useful work. With this design principle, the actuators become variable capacitors charged/discharged during actuation. Since the electrostatic force depends on the accumulated charge, in theory, no more current/energy input is needed to maintain the actuated status of the actuators. Despite very low leakage currents due to fabrication imperfections, the induced energy loss is often negligible (Acome et al., 2018). This difference in the actuation principle significantly improved energy efficiency during bio-mimetic tasks such as standing and cargo holding.

A few different designs under the electrostatic actuator category represent the current state-of-the-art progress in actuator research. Dielectric elastomer actuators (DEAs) (O'Halloran et al., 2008) were constructed with alternating layers of elastic insulators (dielectric) and conductors (electrodes). When a voltage is applied across the actuator, charge accumulation on the electrodes results in electrostatic forces that compress the elastic insulator layers. Axial compression as well

as radial expansion could be observed. This compression allowed the actuators to be used in both contracting and expanding applications. However, the main challenge ahead of DEA researchers is that it is not straightforward to integrate the actuators into robot prototypes. Not only was it hard and expensive to manufacture stacks when more layers were involved in high-strain tasks, but their fully soft nature also required extra design efforts to connect the load to the actuators. Since the electrostatic force is inversely proportional to the thickness of the insulator material, it was also challenging to fabricate actuators with high-stress and thin insulator layers as thinner insulator layers would lead to higher probabilities for electric breakdowns during actuation.

Another front line of research targeted actuators with flexible materials that bend when electrostatic forces are applied. Electrostatic zipping actuators use the electrostatic attraction between electrodes to zip two electrodes toward each other gradually. This creates contraction forces that can be easily utilized by rigidly attaching the load to one of the electrodes. Further addition of a small amount of dielectric liquid between the zipping electrodes significantly increased the dielectric constant between the electrodes, which increased electrostatic forces. The liquid dielectric can be compressed into a thin layer which further aided the generation of higher actuation forces. The working principle of such actuators is provided in Fig. 1. Taghavi et al. (2018) demonstrated this technological pathway's potential with various actuator prototypes, which reached up to 5N pulling forces and up to 98% of strain. The prototypes showed very good strain data based on the thickness of the actuators. However, it is worth noting that the larger width of the actuators and their effects on future integration were not discussed in detail. The addition of dielectric liquid also brought forward challenges in constraining the liquid within the actuator during longer-term applications. A full enclosure around the actuator could be a possible solution but would also be heavily limited by the width and length of the actuator structure.

Hydraulically amplified electrostatic actuators represent the latest developments in electrostatic actuator technology. Those actuators featured a design where electrostatic forces were amplified hydraulically in sealed pouches filled with dielectric liquids.(Rothemund et al., 2020)(Kellaris et al., 2019) Prototypes were reported to have muscle-like performance (Kellaris et al., 2018). However, fully-filled pouches introduced extra mass into the system, and the hydraulic amplification geometry greatly limited the maximum strain of the actuators. Both concerns limited the potential of hydraulically amplified electrostatic actuators as artificial muscles in mobile autonomous robots.

To summarize, the current actuator technologies have yet to meet the need for further robotic developments. Academia and industry need novel solutions to bring out the full potential of soft robotic technology. This project was thus motivated to explore the potential of such a novel actuator design.

1.3 Our Approach

The proposed actuator shares the same actuation principles as electrostatic-ribbon actuators (Taghavi et al., 2018) but with two helical electrodes arranged into a double helix instead of two flat ribbon electrodes. The proposed design is shown in Fig. 2. The working principle of the proposed actuator is illustrated in Fig. 3. This change in design was inspired by recent developments from Nishimura et al. (2022), where a double helical actuator structure was constructed and tested. Double helical structures were initially proposed by Carpi et al. (2005), but only as DEAs. Nishimura et al. (2022) changed the structural material into flexible photosensitive resin and added liquid dielectric (A liquid crystal material developed in-house) to improve performance. A strain of 19% was observed with only 200V applied. The fabrication and testing of the helical actuator were provided in Fig. 4. As an insulating spacer also in the form of 3D printed photosensitive resin was included in the design, it is possible that replacing the spacer with a much thinner coating will allow the actuator to contract further. This might further increase the maximum strain of the actuator to be above 30%. Since electrostatic forces are inversely proportional to the distance between electrodes, a thinner insulating layer will also produce larger actuation forces. Taghavi et al. (2018) demonstrated an actuator prototype capable of 5N contraction forces while being only 10mm wide. This showed further potential in the proposed actuator since a helical design can allow for wider electrodes thanks to improved compactness.

1.4 Goals

The goal of this thesis project is to provide initial verification of the proposed actuator technology, it includes the design, fabrication, and testing of the proposed electrostatic actuator. In the beginning, a fabrication process will be developed and documented to fabricate actuator prototypes. A series of prototypes will then be developed to explore the potential of the actuator concept as well as its application in a robotic setting. The performance of the actuator will be evaluated by force and strain measurements.

1.5 Contributions

This thesis project aims to contribute to the robotics community with a principle study around an innovative actuator concept. The knowledge and experience gained in the design, fabrication, and testing of such actuators can provide insights into future improvements in electrostatic actuator technology. Targeting a strain of 30% and contraction forces of up to 5N within a compact package, the proposed actuator will combine the benefits of hydraulically amplified electrostatic actuators (high force but low strain around 10%) and ribbon actuators (high strain but bulky). The proposed actuator concept will provide researchers and engineers with a powerful flexible actuator to use in future bio-mimetic robot designs. An actuator comparable to a human bicep in strain and size will be the target result. This will greatly simplify the integration of such robotic systems into humanoids and quadrupedal robots, moving one step closer to building robots that are just as good as those created by nature.

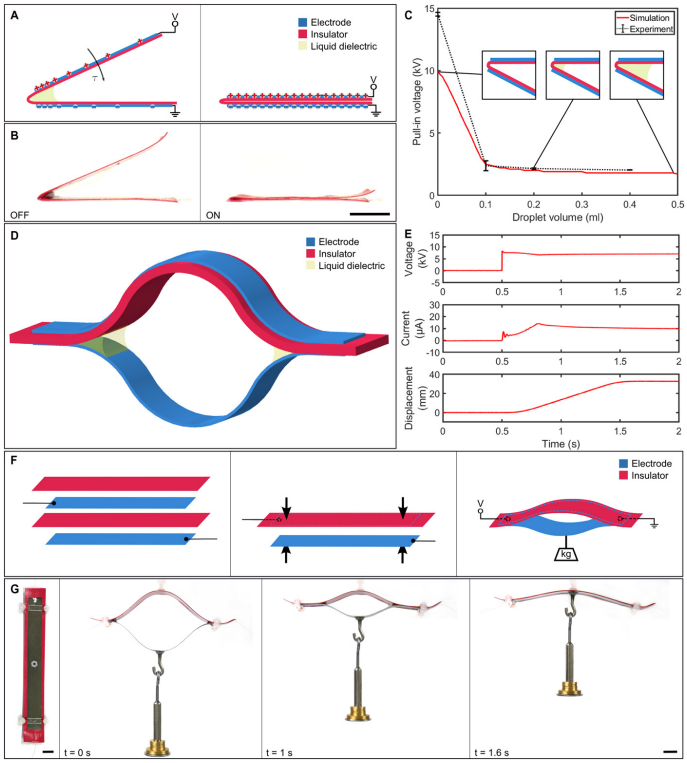

Figure 1: Principle of the ribbon actuator. A small amount of dielectric liquid enhances the electrostatic force, resulting in better performance of the resulting actuator. Figure adapted from Taghavi et al. (2018).

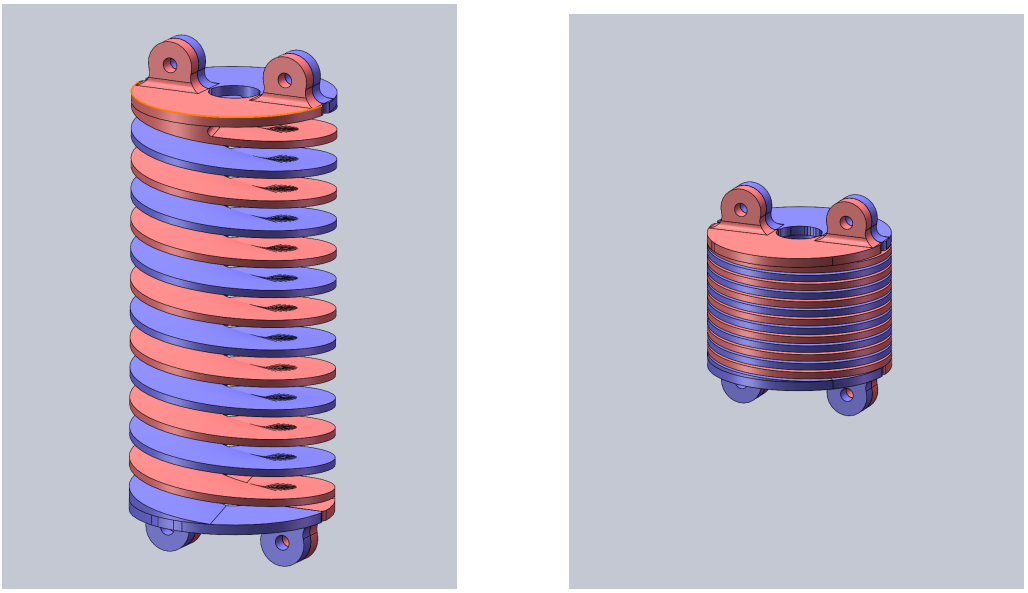

(a) Initial (Open) state of the proposed actuator. (b) Actuated (Closed) state of the proposed actuator.

Figure 2: The proposed actuator design. Blue and red indicate two non-touching electrodes with opposite polarity.

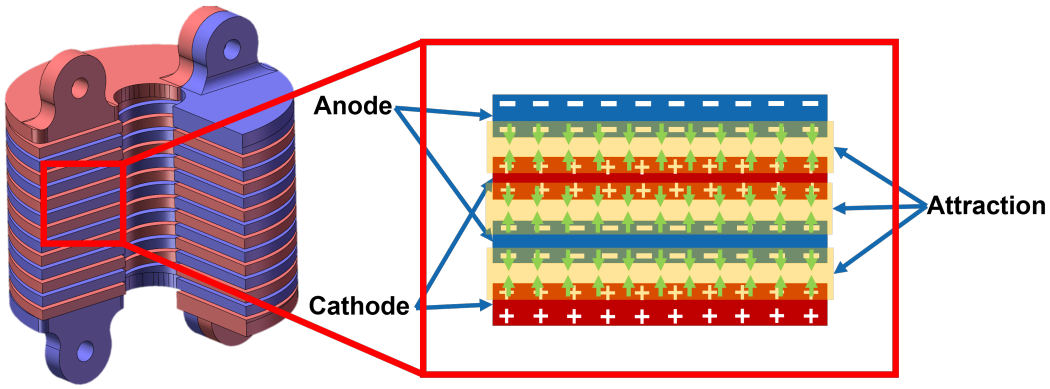

Figure 3: Cross-sectional view of the proposed actuator design. Blue and red indicate two electrodes with opposite polarity. Charges accumulate when a high voltage is applied between the two electrodes. Attractive electrostatic forces act on the two electrodes and compress the helical structure, resulting in useful contraction work.

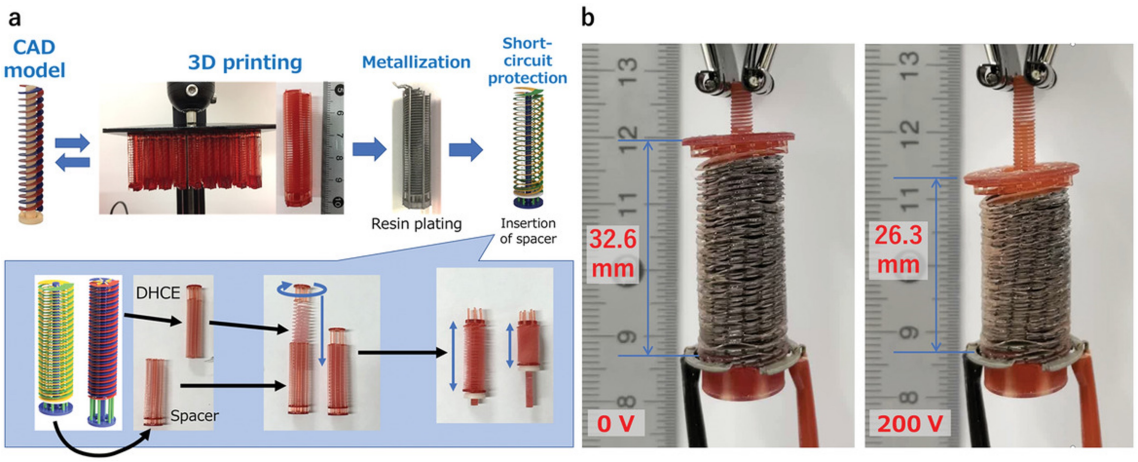

Figure 4: Fabrication and testing of the double-helical actuator adopted from Nishimura et al. (2022). Note the spacer which serves as insulation between the electrodes.

2 Methodology

This section aims to provide information regarding the execution of the thesis project. The methods used are described in detail for the repetition of experiments by future researchers. A brief discussion of the method selection process is provided where necessary. Challenges encountered during project development are also discussed.

The successful execution of the thesis project was made possible by efforts and results in the following areas: Material, Structure, Insulation, Manufacturing, and Experiments. Each aspect was crucial for the development of the next aspects of the project. Those aspects are thus discussed following the sequence by which they were developed during the thesis project.

2.1 Materials

Before starting the development of the Double-Helix ElectroStatic Actuators (DHESA), it is important to briefly revisit the proposed working principle of such actuators to identify key functional requirements. The proposed DHESA should mainly consist of two helical electrodes that are twisted together to form a double helical structure. Each electrode serves two major functions: maintaining structural integrity and electrostatic actuation functionality. This means that the electrode material selected should be rigid enough to ensure support of the actuator structure and weight. The selected material should also ideally be conductive. This is because otherwise extra manufacturing steps will be required to improve conductivity for electrostatic actuation. Apart from the above functional requirements, the helical structural requirement also complicates the fabrication process and imposes further constraints on material selection.

Two aspects were considered during material selection. First, materials were selected based on their manufacturing flexibility. This is again due to the complicated geometry of the proposed electrode design. Possibilities of conductivity enhancements were then discussed for the selected materials to finalize material selection.

2.1.1 Shape Forming

Since the actuators take advantage of the double helix design, conventional subtractive manufacturing techniques such as milling and turning cannot be used to fabricate the helical electrodes. This is due to challenges in the proper fixture of the thin-walled helix during material removal. The costs associated with custom molds/fixtures involved in conventional fabrication methods are also beyond the scope of this thesis project.

On the other hand, additive manufacturing (AM) techniques such as 3D printing are more fitting

thanks to the wide range of available materials and the ability to fabricate complex geometries with ease. 3D printing is thus selected as the primary means to form the basic shape of the actuators. There are 4 major varieties of 3D printing technology, namely Fused Deposition Modeling (FDM), Stereo Lithography (SLA), Selective Laser Sintering (SLS), and Selective Laser Melting (SLM).

The SLM process uses high-energy laser beams to selectively melt layers of base material in a fine powder form. This process directly produces components with a wide selection of metals including copper, gold, and titanium. This meana that the resulting components will be natively conductive and a further plating step can be omitted. Furthermore, the SLM process can produce parts with very accurate dimensions and a powder-based printing process also reduces the need for support structures. This makes SLM the best choice for the proposed project. However, the SLM process requires industrial-class equipment and the material cost is also beyond the budget scope of this project. Hence, other technologies are prioritized.

SLS technology, where laser beams are used to selectively sinter powdered materials in a layered fashion, shares similar principles as the SLM technology, but the base materials more commonly consist of plastics such as Nylon. Since SLS shares the same equipment and budget limitations as the SLM process, this leaves only FDM and SLA technologies as the available fabrication process for this project.

FDM technology involves the controlled extrusion of melted plastic material to form pre-defined 2D sections. Although simpler and much more widely available, FDM produces components with an uneven surface due to the layered construction. The minimum layer height is also limited to around 0.1mm due to thermal limitations. When printing with thinner layers, the previous layers also melt which disturbs printing accuracy. The requirements of removable supporting structures also leave a much rougher and unpredictable bottom surface on all the helix structures. Since the fabricated components will need to go through further plating and coating to form the final electrodes, the increased roughness produced by FDM is undesirable.

SLA technology involves controlled laser scans to selectively activate photosensitive resin materials to form layers that shape into the final component when stacked. The minimum layer height can be reduced to 0.05mm thanks to the reduced number of moving parts during the construction process. The focused laser beam can also reduce the minimum pixel size within each layer which further improves the resolution and accuracy of the final product.

With the above discussions and analysis, it is clear that the SLA process should be the primary process used to form the basic shape of the Helical electrodes. Throughout the project development, a Form3 resin printer from Formlabs was used to produce all samples with default settings and a 0.1mm layer height.

Before printing the helical electrodes, a few preliminary tests were carried out to select the best-fitting material in the Formlabs resin catalog. The materials tested were selected based on function and availability. The resin material tested exists in Durable, Clear, ESD, and High-Temp versions. Those resin materials were all proprietary offerings from Formlabs.

Flat-ribbon electrodes were designed and test-printed with each resin. The main reason to test with flat ribbon actuators was the ease of insulation and assembly, which later proved to be very challenging with helical electrodes. The flat ribbon design was also easier to print and generated less material waste thanks to the reduced amount of support structure. A picture of the printed electrodes is shown in Fig. 5.

After printing and post-processing (washing and curing) following standard guidelines provided by FormLabs, the rigidity as well as strength of the materials were examined by manually bending the electrodes and observing the elastic deformation.

The durable resin, although very resilient and easy to print, proved to be too soft and can be easily deformed plastically. The High-Temp resin on the other hand proved to be too hard and brittle, cracking and shattering upon bending. This left only Clear and ESD resin to be further evaluated.

To verify the functionality of the electrodes, copper tape was applied to the electrodes to provide a conducting surface. A layer of insulation was added on top before two electrodes were assembled

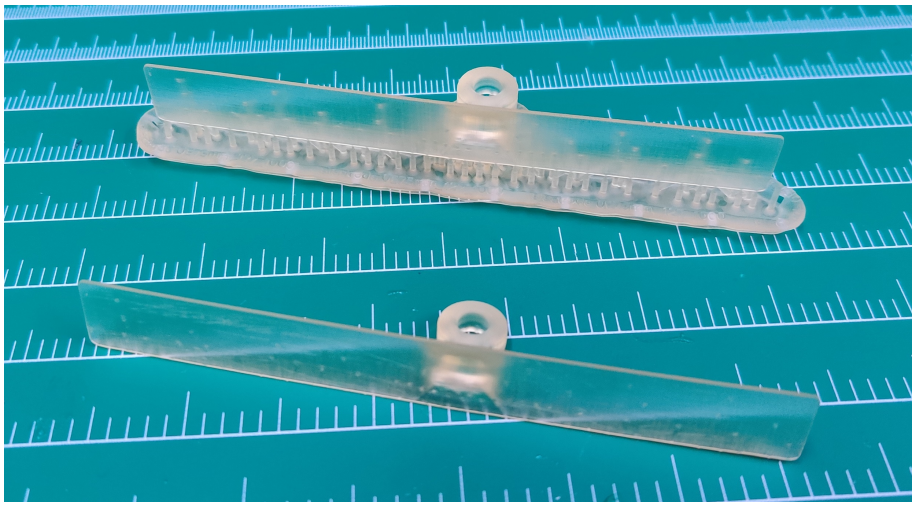

Figure 5: Flat electrodes printed with the High Temp Resin (Photosensitive resin from FormLabs, capable of surviving temperatures up to 238°C). Top and bottom shows the electrode before and after post-processing.

into a test actuator. The details of the tests will be covered later in 3.1.

Having similar mechanical properties, the Clear and ESD resins showed similar results when tested in an actuator. Actuator samples made with both materials showed similar movement when charged with a high voltage. Although the ESD resin required more effort in the washing step, it was selected over the Clear resin thanks to its conductivity benefits.

After ESD resin was selected as the electrode printing material, a few helical electrodes were printed. It turned out that the printing orientation played a key role in the final quality of the printed electrodes. Two orientations(shown in Fig. 6) were tested and compared.

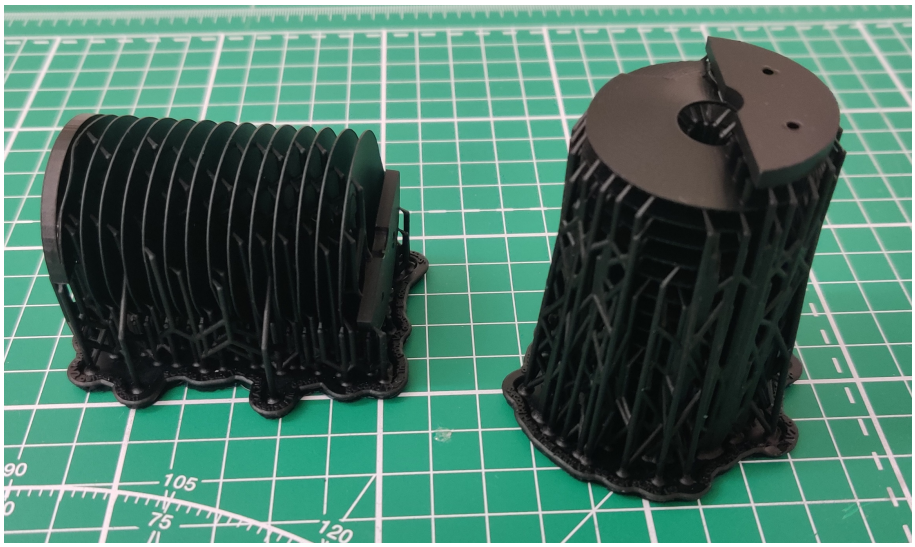

Figure 6: Two printing orientations. The lying-down orientation is shown on the left and the upright orientation is shown on the right.

The upright printing orientation was tested first with hopes for a smoother and more consistent helical structure. Support structures were critical in ensuring successful and consistent printing quality, but left irregular connection points on the supported surface. Since the inner surfaces of the helical electrode had to be insulated later with a thin insulation layer, it was ideal to keep those surfaces smooth and free of support. It was thus challenging to lay out the support structures

around the upright helix. The slicing software (PreForm) provided by FormLabs could not impose surface constraints during automatic support generation. This was solved by adding dedicated support pillars directly in the design, as shown in Fig. 7. The support pillars are attached only slightly to the helix and could be easily cut off after printing. This allowed the successful printing of the helical electrode in an upright orientation. However, further examination indicated that the helix cross section deformed during printing, and the electrode thickness was much higher than designed. This was believed to have resulted from the repeated lifting and lowering of the printing platform during the printing process. With a limited amount of support and a softer helical structure, the helical electrode deformed repeatedly with every layer, and accuracy with electrode thickness was affected. This unwanted deformation also left a very rough bottom surface across the entire helix which could not be smoothed with post-processing.

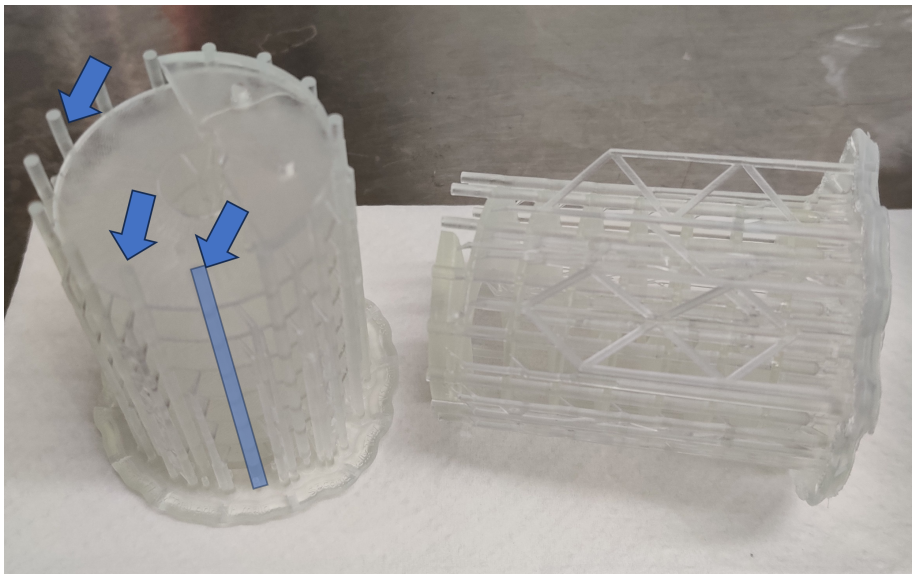

Figure 7: Helix printed with support pillars. Arrows indicate the support pillars, those are included in the design file and removed after printing.

The other possible orientation had the helix lying down on its side during printing. This option was not prioritized due to worries that the layer lines would result in printed helices that are not radially homogeneous. This disadvantage proved to have less effect on the printing results as long as the electrode thickness exceeded 0.5mm. Automatically generated support structures only had to be slightly tweaked away from the internal surface of the helix before an electrode could be printed. This change of orientation also significantly simplified the post-processing of printed electrodes thanks to the reduced amount and complexity of support structures. The uneven interface created by the support could be easily trimmed with a drill bit or sanded off with sandpaper. Those results finalized the shape-forming process which involved the SLA printing with ESD resin of helical electrodes in a side-ways orientation.

2.1.2 Conductivity Enhancements

Explorations in conductivity enhancements were carried out in parallel with the development of the shape-forming process. This was originally planned as a backup option to enable non-conductive materials. Although this step was proven not necessary in the finalized fabrication process, documentation and discussion are still provided here to serve as a reference for future researchers.

A few methods exist to improve the conductivity of the printed electrodes. Firstly, conductive additives can be mixed into the photosensitive resin to improve the conductivity of the printed parts. Such additives include graphite, carbon nanotubes, silver nanoparticles, and silver nanowires. Most commercially available conductive resins are developed with this method which proves its effec-

tiveness. However, since the additive also affectes the printability of the base resin and requires research efforts in tuning, this possibility is excluded from this thesis project.

Another way to improve the conductivity of the electrodes involves coating/plating a layer of conductive material on the surface of the electrodes. There are mainly two types of conductive materials that can be plated/coated. One involves materials containing carbon, such as graphite, carbon nanotubes, and graphene. The other involves various metals such as copper, gold, and nickel. The different material formulations lead to different application processes.

The coating of carbon-based materials is usually done by painting/spraying a mixture consisting of carbon material, a bonding agent, and an organic solvent such as Methyl Ethyl Ketone (MEK) and Acetone. Several available conductive paints are shown in Fig. 8. As the solvent evaporates, the bonding agent and the carbon material form a conducting solid layer on the surface of the part being coated. One major concern of this type of application process is the inclusion of organic solvents. In the later step of insulation, a similar process will be used to coat insulating materials on top of the conducting layer. This insulating process will also involve strong solvents such as MEK, which might dissolve the bonding agent underneath during the insulation coating step and lead to unpredictable outcomes. One potential risk will be that the structure of the insulation layer can be compromised due to deformations in the conducting layer. This will lead to defects and eventually premature electrical breakdown during operation at high voltages. Carbon-based materials are thus given less priority in the coating process.

Figure 8: Three available conductive paints. From left to right: copper-based Lumilor backplane BP-B311, carbon-based carbon paint DAG-T-502, and carbon-based paint CI-2051.

Metallic materials can be applied in three fundamentally different processes. The first process is very similar to the application of carbon-based materials involving solvents and bonding agents, the only difference is the replacement of carbon-based materials with fine metal particles. It will thus share the same process limitations as carbon-based materials. Two other processes involve chemical/physical reactions to deposit metal atomically on the surface of the component being plated. Both of those two processes will be capable of forming a layer of metal on the component's surface, which will be resistant to the solvents used in later steps. Depending on whether an external electric current is involved, the two processes are named electro-plating and electroless plating.

Electroplating involves a flowing current between the components and sacrificial anodes made with the target plating metal. Metal ions in the electrolyte submerging the component get deposited on the surface of the component and replenished from the atoms on the sacrificial anode. The main disadvantage of electroplating is that the components need to be preprocessed with other methods such as carbon painting if the component was made of non-conductive materials such as resins used in the SLA process. Another factor that limits the electro-plating process is surface

quality. Since the metal ions get deposited following the current flow, uneven current flow in the plating process can lead to non-uniform plating thickness. The counter to this limitation requires careful tuning of the external driving voltage and the component being plated also has to rotate slowly so that all surfaces receive equal plating. A plating system consisting of an electrolyte tank, two copper electrodes, and a rotating fixture was constructed (shown in Fig. 9) but was not tested since this step was later proved unnecessary.

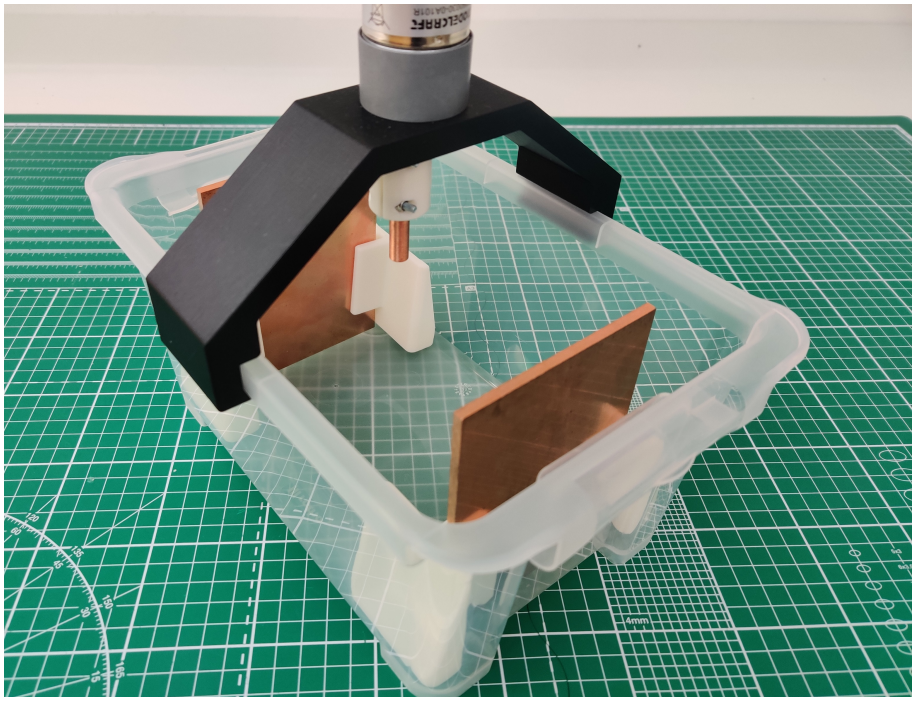

Figure 9: Electro-plating setup. This setup includes a tank for electrolytes, two copper plates as anodes, and a rotating copper mount for cathodes.

Electroless plating, as the name suggests, does not require an external power source. A series of chemicals are specifically formulated to treat the surface of the component before it is placed in a plating bath containing ions of the target metal. At the correct temperature and pH, a self-catalytic reaction deposits metal ions on the surface of the component. This process forms a dense and uniform plating layer on the surface and does not have specific conductivity requirements for the base material. A commercial plating kit (From Caswell, shown in Fig. 10) was purchased and tested. The plating was not successful despite following standard guidelines provided by the manufacturer. The failure is demonstrated in Fig. 11. The possibility of material incompatibility was ruled out with similar failures when plating the provided sealer resin. Potential explanations for the failures include low temperature and material expiry, but further investigation is omitted as the ESD resin proved functional by default.

2.2 Structure

This section documents the iterations regarding the base structure of the actuators during project development. Design modularity and form factor are the main areas where optimization was carried out.

2.2.1 Design

Despite a straightforward working principle, the structural design of the actuator is complicated. Since the actuator works under high voltage in the range of kVs, careful design considerations have to be made to ensure proper insulation. The electrodes must be insulated from each other to prevent electrical breakdowns and actuator failure. They must also be insulated from the outside

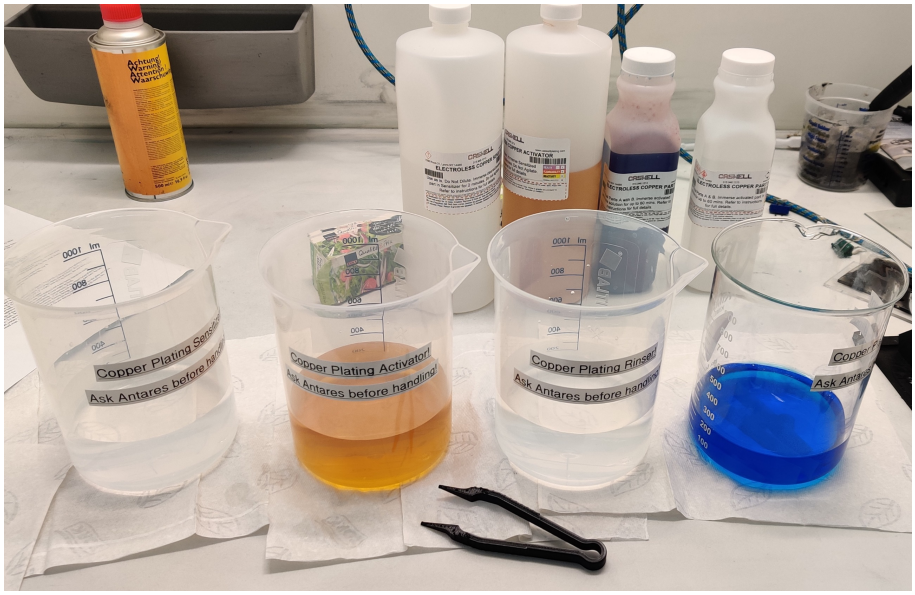

Figure 10: Electro-less-plating setup. The sample is sequentially treated in the sensitizer, activator, and plating solution.

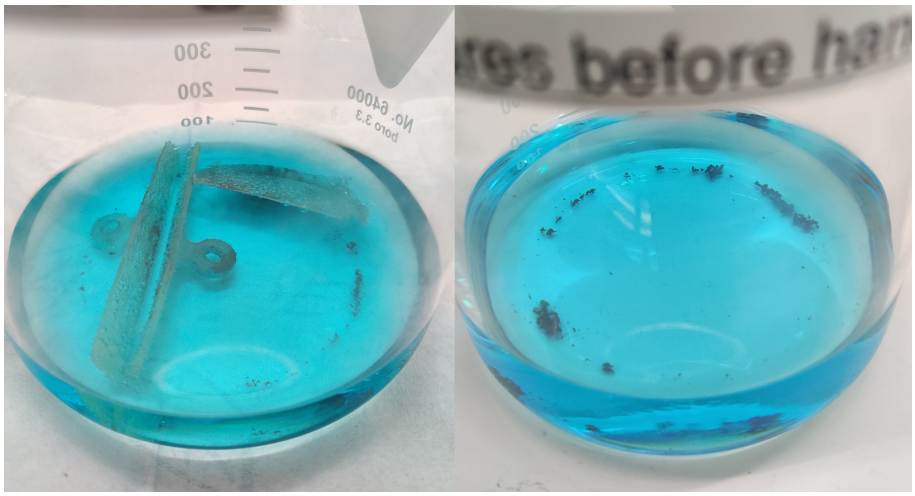

Figure 11: Failures in the electro-less-plating tests. The samples are not fully plated on the left and copper precipitation can be observed on the right.

environment, especially the fixtures that connect the actuators to the robot, to maintain safety during operation. Another aspect to consider is to minimize the need to deform the electrodes during assembly. This is to avoid damaging the insulation layer on the surface of the electrodes.

The first generation of the actuator design featured helical electrodes that combined with the fixtures of the actuator. This generation was mainly designed to verify the printing process of the electrodes. The version 1 design is shown in Fig. 12. After printing, the two identical helical electrodes were twisted together to form the actuator. This version did not fully consider the insulation and the two electrodes were touching at both ends of the helix. This posed a high risk of electrical breakdowns and was improved in the next version. Also, due to the thickness of the fixture structure at both ends of the helical electrode, the helical section of the electrodes had to be stretched open wider during assembly. This created two potential problems with the finished actuator. Firstly, this could overstretch and permanently deform the electrode structure. Secondly, there was the risk of the insulation layer being scratched and damaged by the protruding fixture structure. The above concerns led to design changes in the second version of the electrode design.

The second version was designed with improved modularity, easier assembly, and better insulation. It mainly featured modular separation of the electrodes and the fixtures at both ends. Two insulating spacers were also added at both ends of the actuator to separate the fixtures and serve as external attachment points of the actuator. The version 2 design is shown in Fig. 12.

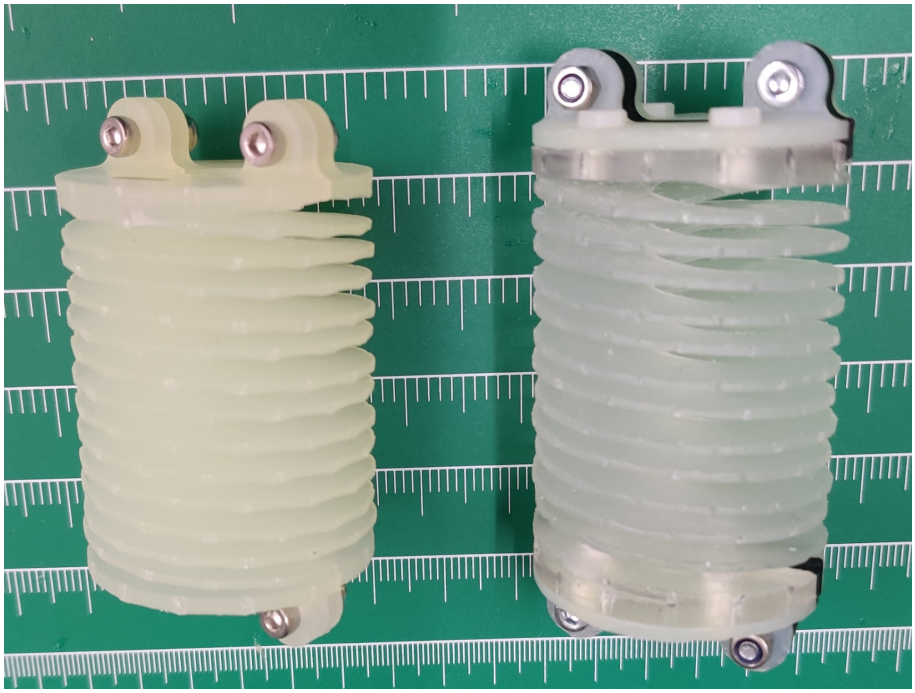

Figure 12: Two versions of the electrode design. Version 1 is shown on the left, notice the combination of the helical electrode and the fixtures at both ends. Version 2 is shown on the right, notice that the fixtures are separated and black insulating spacers are also added.

With the improved second version design, the electrode thickness was significantly reduced and actuator assembly could be done without large deformations of the electrodes. Tapped holes were added at both ends of the electrode to connect to the fixtures during assembly. After the electrodes were twisted together, the fixtures could be attached with insulating nylon bolts. Finally, the insulating spacers were printed with PLA and attached to the fixtures with bolts to finish the assembly.

All helical actuators tested in the thesis project followed the updated version two design principles and only the actuator dimensions (radius, thickness, pitch, number of loops, etc.) were varied.

2.2.2 Form Factor

Another very important design consideration is the form factor of the actuator/electrodes. Trade-offs have to be made between dimensions such as inner diameter, outer diameter, functional length, and electrode thickness. Since the electrostatic force scales proportionally with the effective area of the actuators, it is beneficial to have helical electrodes with a larger outer radius and smaller inner radius. This configuration will maximize the ring area in which electrostatic zipping happens during actuation, giving higher actuation forces. However, since the total volume/weight also plays a key role in determining the energy/power density of the actuators, the maximum outer dimension of the actuator design has to be limited. Another limiting factor is the available printing volume of the Form3 printer used to fabricate the electrodes, which is 145x145x185mm. The functional length of the actuator is defined to be the pitch of the helix multiplied by the total number of loops in the helix. This dimension will affect the amount of contraction the actuator can make when powered.

The first generation of helical electrodes were designed with 50mm outer diameter, 10mm inner diameter, and 15 loops with a 4mm pitch. The assembled actuator had the outer dimensions of a pillar with 50mm outer diameter and 60mm height. This was intended to imitate the size of the biceps muscle in the human body. The insulation process of the first-generation design was problematic due to the higher number of loops in the helical electrodes. Since the insulation was done manually, the increased number of loops required more effort and also increased the chance of defects during insulation. The only benefit was potential improvements in maximum strain thanks to the increased length of the actuator. However, this was not necessary in the proof of concept stage of the project. The number of loops was thus reduced in later designs.

Another design iteration happened with the electrode thickness and pitch of the helix. The first generation of the electrode design had the electrode thickness at 1mm and the pitch at 4mm. This meant that there was still a gap between the electrodes after assembly. The size of this gap can be calculated as (pitch - 2 x electrode thickness)/2, which was 1mm in this case. The initial consideration for such a design choice was to leave more room for the electrode to contract during actuation. However, upon manual examination of the finished actuator, concerns were raised that the electrostatic force would have to overcome the internal spring forces to achieve full zipping during actuation. It was soon realized that the spring forces in the original ribbon actuator design played a key role in actuation force improvements. The electrodes did not separate by default and were pulled open when an external load was added. The elastic spring force of the electrode structure was then used to assist during actuation. With such conclusions, the gaps between assembled electrodes in later versions were removed.

The final design change was driven by the insulation process. After testing various insulation methods, the most reliable process found was the manual application of film tape made with Kapton. The details leading to such findings will be covered in 2.3.1. Manual application, although requiring practice and effort, was able to create an insulation layer that could withstand voltages higher than 5kV. Kapton tape was manually added to the first-generation electrodes, but the 10mm inner diameter of the electrodes created challenges for the application process. Since the available space was too small, the tape covering both sides of the electrode couldn't be joined together in the middle. This left open sections on the insides of the electrodes, which resulted in premature breakdowns when voltage was applied. To tackle this issue, an updated design with 70mm inner diameter and 120mm outer diameter was used. The larger 70mm inner diameter gave enough space for the Kapton tape to be joined in the middle. There was also enough space to overlap the tape for 10mm which further improved the insulation.

2.3 Insulation

Electrostatic actuators rely on electrostatic attraction forces to generate useful work, the generated force is proportional to the square of the applied electric field as more charge can be accumulated with higher driving voltage. It is important to keep the two attracting electrodes insulated as otherwise electrical breakdown will occur. Such breakdowns will not only stop the force generation by clearing accumulated charge but can also result in arcing and lead to catastrophic failures in the

actuator structure. Indeed, a rapid discharge in the actuator will result in very high instantaneous currents that will permanently damage the actuator structure and can even cause a fire hazard in severe cases. It is thus important to ensure full insulation between the two helical electrodes proposed in this project.

A few different methods are used to provide insulation between electrodes in electrostatic actuators. DEAs use intermediate elastomer layers as insulation, HASELs use structural film layers as insulation, and electro-ribbon actuators use PVC tape as insulating layers. Different material and insulation processes play an important role in the performance and stability of the final actuator prototypes. There are three ways the insulation can affect the actuator's performance. The electrostatic driving force of the actuator is proportional to the dielectric constant of the insulating material and inversely proportional to the thickness of the insulation layer. The maximum driving voltage of the actuators is determined by the breakdown strength as well as the thickness of the insulating layer. For actuators with higher performance, an ideal insulating solution should be a thin layer of high dielectric constant material fully encapsulating the electrodes.

2.3.1 Film/Tape Application

It is common practice in the electronics fabrication industry to insulate delicate electronics with insulating tape/film made with Kapton (polyimide) or PVC. The electro-ribbon actuators that inspired the idea leading to this thesis project are also insulated with conventional PVC tape and verified to work. With proven success and potential, the application of insulating tape was then tested and evaluated.

Different tape/film materials were applied to the flat-ribbon actuators used for material selection. Conventional insulation tape (PVC), 12um Mylar (PET) film, and 25um Kapton (polyimide) tape were tested. Flat-ribbon actuators tested with those insulating tapes are shown in Fig. 13. The different tapes/films were evaluated by their ease of application and their stability when applied. The Mylar film didn't have adhesive but featured a heat-sealable adhesion layer and was proven effective in various electrostatic actuators(Kellaris et al., 2018). However, heat-sealing would be challenging when used in the complex helical structure. Attempts were made to wrap the Mylar sheet around the flat-ribbon electrode but were unsuccessful. PVC tape on the other hand had an adhesive glue layer and was stretchable to fit the geometry of the electrode. However, the thickness of the PVC tape was higher than Kapton tape and the adhesive also had weaker bonding than the adhesive of Kapton tape. PVC tape detached easily especially after the dielectric oil was added. Finally, Kapton tape had the best performance of the three evaluated insulation materials. The Kapton tape was available in various sizes and thicknesses and was also slightly stretchable. The adhesive on the Kapton tape was also more stable and could withstand the dielectric oil without losing adhesive capabilities. Kapton tape was thus selected for all future fabrication and experiments.

2.3.2 Polymer Coating

The current state-of-the-art insulation solution involves coating electrodes with a very thin layer of PVDF (Della Schiava et al., 2020). This is achieved by first dissolving the PVDF polymer in a solvent (MEK) to create a solution which is then coated onto the electrodes with blade coating to create a very thin layer (5um). As the solvent evaporates, the PVDF polymer is left on the surface of the electrode as a thin insulating layer. The layer thickness can be altered by adjusting the concentration of the PVDF solution. The PVDF insulation has very high potential thanks to the significantly higher dielectric performance when compared with Mylar (Kellaris et al., 2018), Silicone (O'Halloran et al., 2008), and PVC, respectively used in HASELs, DEAs, and electro-ribbon actuators. There exist mainly two types of PVDF polymer that can be used as insulation. P(VDF-TrFE-CTFE) Terpolymer has a very high dielectric constant but is limited by material availability and breakdown strength. PVDF-HFP has lower dielectric performance but is much more available and also has better mechanical and breakdown strength. Since the proposed project mainly focuses on the feasibility study and not performance optimization of the helical actuators, PVDF-HFP is selected as the insulation material for the helical electrodes.

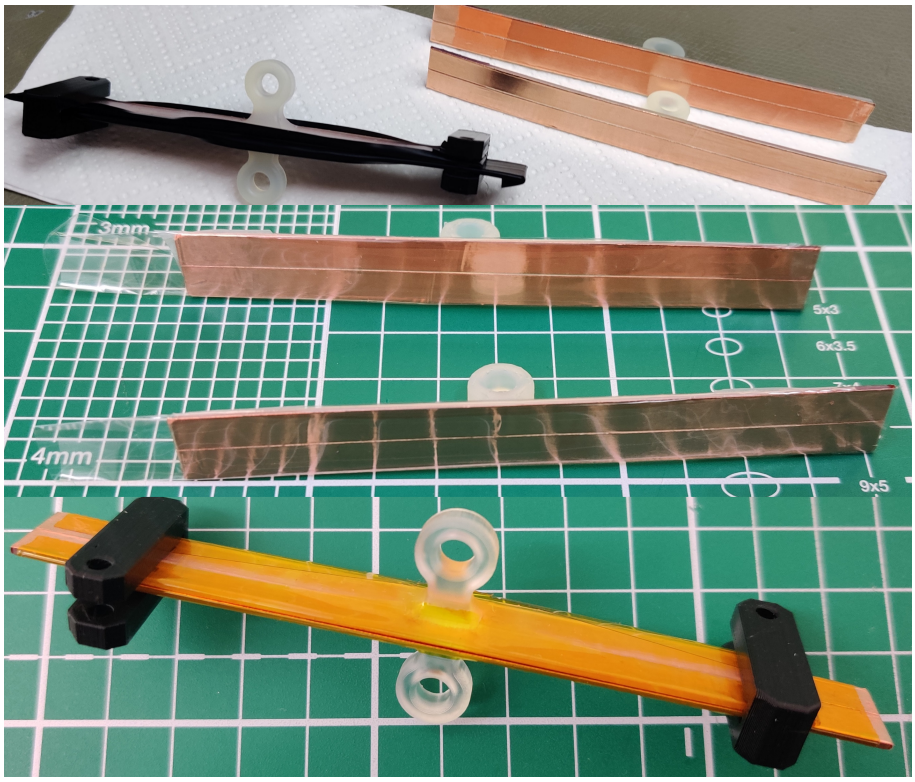

Figure 13: Flat-ribbon actuators insulated with different insulating materials. From top to bottom: PVC tape, Mylar film, and Kapton.

The above-mentioned insulation solution is adapted for the proposed project. The complex surface of the double helix electrodes makes it impossible to apply the coating with conventional blade-coating techniques. A few possible coating techniques exist and are evaluated. Potential techniques include dip-coating, spray painting, and spin coating.

Dip coating is commonly used in the industry to apply a surface coating to components with complex geometries. This is done by fully dipping the component in the coating solution, composed of the insulating material (PVDF) dissolved with a solvent, and then slowly pulling out the component following tuned speed profiles. When executed correctly, a layer of insulating material will be left on the surface of the component. Different coating layer thicknesses can be achieved by varying the concentration, i.e. the viscosity of the coating solution. The challenges that arise from such processes include tuning of pull-out speeds and uneven coating thickness due to fresh coating accumulation at the bottom sides of the component.

Spray painting involves spraying the surface of the component with the coating substrate. Different layer thicknesses can be achieved with multiple applications of the spray-painting process. The spray-painting process can adapt well to uneven surfaces but is less effective in the coating of internal geometries and hard-to-reach areas such as inside deep groves or holes. The double-helix electrodes proposed in this project will not have a very high pitch angle as the higher zipping angle will otherwise reduce the available force of the actuators. This low pitch angle means that the helixes will be densely packed, resulting in great difficulty in reaching the top and bottom surfaces in the middle of the helical structure. This limitation makes spray painting an inferior method compared with dip coating.

Spin-coating is very commonly used in the semiconductor industry where very thin layers of resin are applied on wafers in the chip fabrication process. The coating material is dripped onto the center of the base material while the material is spun at a very high speed of several thousands of rpm. The centrifugal acceleration will then spread and level the coating material. Extra material is spun off at the edges and a thin layer of coating material is left on the wafer. The coating

thickness can be adjusted by the coating material concentration and the spinning speed.

Since the helical electrodes will have a circular profile, spin-coating will be a very good fit for the insulation of the electrodes. However, since the helical electrodes have a 3-dimensional structure, initial coating material deposition cannot be done by dripping the coating material onto the helix. Taking inspiration from the dip-coating process, a hybrid process called dip-spin-coating is developed for the project.

The dip-spin-coating process combines the material deposition process from dip-coating and the material distribution/removal process from spin-coating. The base material (helical electrode in this case) was first dipped into a solution of PVDF-HFP, this covered the entire surface of the electrodes with the PVDF-HFP solution. The dipped electrode was then spun like the spin-coating process. This spread the PVDF-HFP solution, and excess material was spun off the outer edge of the electrode. A thin and even layer of PVDF-HFP solution was left on the surface of the electrode. After the evaporation of the solvent, an insulating layer of PVDF-HFP was left on the electrode finishing the insulation process.

There exist commercial spin-coater machines used for semiconductor fabrication. However, such machines cannot be used for the project as there is no way to attach the helical electrodes to the spinner properly. Conventional spin-coaters are designed for "2-dimensional" materials such as wafers and cannot adapt to 3-dimensional materials. For this reason, a custom spin-coater machine (Shown in Fig. 14) was developed for the insulation of the helical electrodes. The prepared electrode was installed into the modular coating cage and then attached to the spinner. The spin-coater was powered by a DC motor and the helical electrode was spun together with the coating cage in a repurposed glass jar. The glass jar was used to contain the spinning process and capture any excess PVDF-HFP solution for recycling. The spinning speed could be adjusted by varying the driving voltage of the DC motor. Bearings were installed at both sides of the spinning coating cage for stabilization.

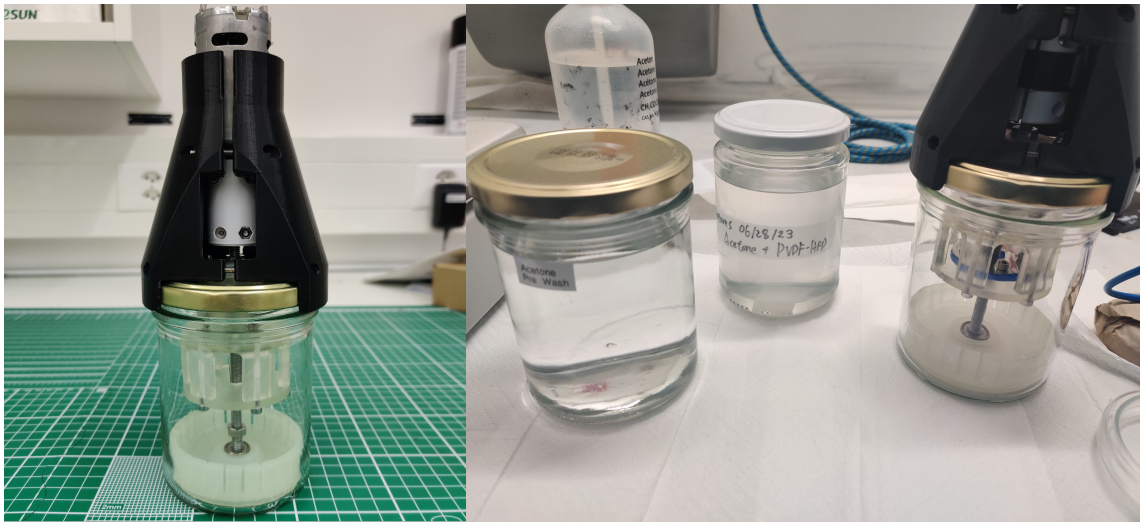

Figure 14: The spinning machine and the dip-spin-coating setup. The samples are installed into the spinning cage, dipped in the PVDF-HFP solution, and spun in the jar.

Since the helical electrodes printed with ESD had a matte black appearance, the visual evaluation of coating quality wasn't straightforward. The evaluation of coating quality was then conducted with aluminum-plated PET sheets. Those were used as the reflective aluminum plating provided a background for visual evaluation. The PET sheets were cut to the same circular shape as the cross-section of the helical electrodes. The PET samples were then fixed to a rigid backing before attachment to the coating cage. Different spinning speeds and spinning times were used. The possibility of stacking coating layers with multiple coatings was also evaluated. Fig. 15 shows some samples coated with dip-spin-coating.

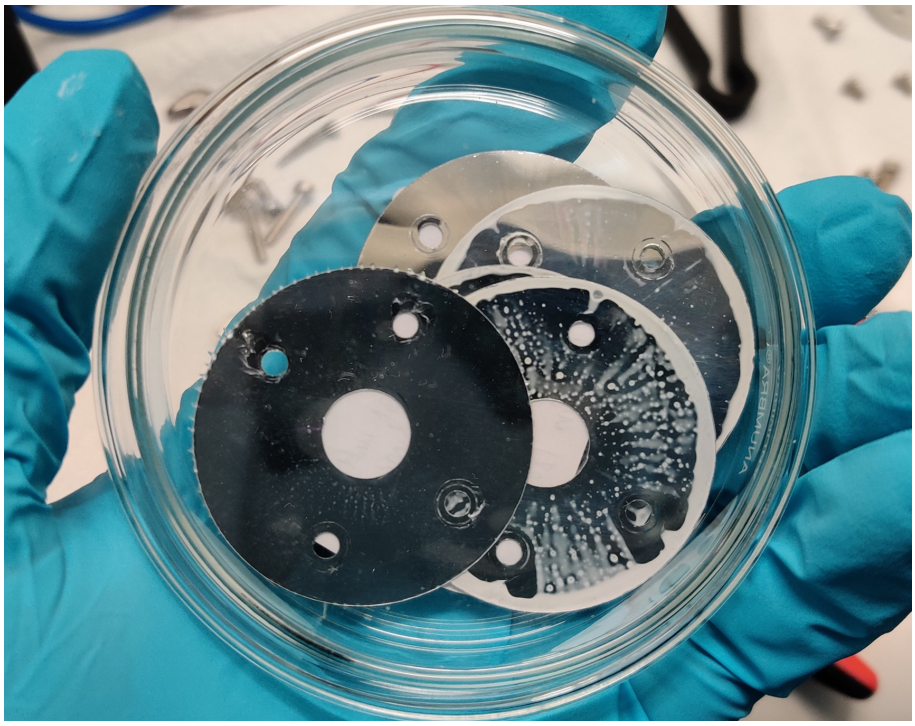

Figure 15: Several PET samples coated with dip-spin-coating and PVDF-HFP. Different speeds and layer counts are used, and the results can be visually evaluated.

The findings of the PET coating experiments can be summarized as follows: Higher spinning speeds will lead to thinner coating layers with higher smoothness. Sufficient spinning time is needed to fully spread the coating solution. Insufficient spinning will lead to uneven coating. Multiple layers of thinner coating will be better than a single layer of thicker coating in terms of evenness. This result is shown in Fig. 16. The completeness of the coating layer was also verified by peeling off the PVDF coating (As shown in Fig. 17) after the solvent (Acetone) was evaporated.

The coating tests done on PET sheets showed good potential as a thick and even coating was achieved by stacking multiple layers of thinner coatings (10 layers of coating spun at 2000 rpm). However, new challenges arose when adapting this verified process to the ESD helical electrodes. The electrode was observed to absorb the acetone used for the PVDF-HFP solution and deform during coating. This resulted in the electrode folding in on itself and caused coating for different sections to adhere to each other. Attempts to separate the adhered coating damaged the coating as shown in Fig. 18. This issue was especially severe during multi-layer coating where the ESD electrode had to be submerged in the PVDF-HFP solution multiple times.

A potential solution for such an issue is believed to be an alternative solvent. The alternative solvent should be a good solvent for PVDF-HFP but should not dissolve or get absorbed by the ESD resin. Since the chemical content of the ESD resin is proprietary and unavailable, the possible options for candidate solvents are limited. Comparing the chemical compatibility and available solvent datasheets provided by Formlabs, Dimethyl sulfoxide (DMSO) was selected and evaluated. DMSO demonstrated good material compatibility as it dissolved PVDF-HFP but didn't interact with the ESD resin. However, the evaporation speed of the DMSO-PVDF-HFP solution was observed to be extremely slow and the DMSO-PVDF-HFP solution covering samples showed no observable volume difference across an hour. Putting the sample in an oven to fasten evaporation was not an option either as the ESD resin is sensitive to temperature. This means that DMSO cannot be used in the dip-spin-coating process.

PVDF Coating experiments were carried out despite the solvent absorbance issue. A temporary fix of reducing the number of coatings and speeding up the coating process was used. This allowed the successful coating of PVDF-HFP onto helical electrodes with a yield of around 50%. However,

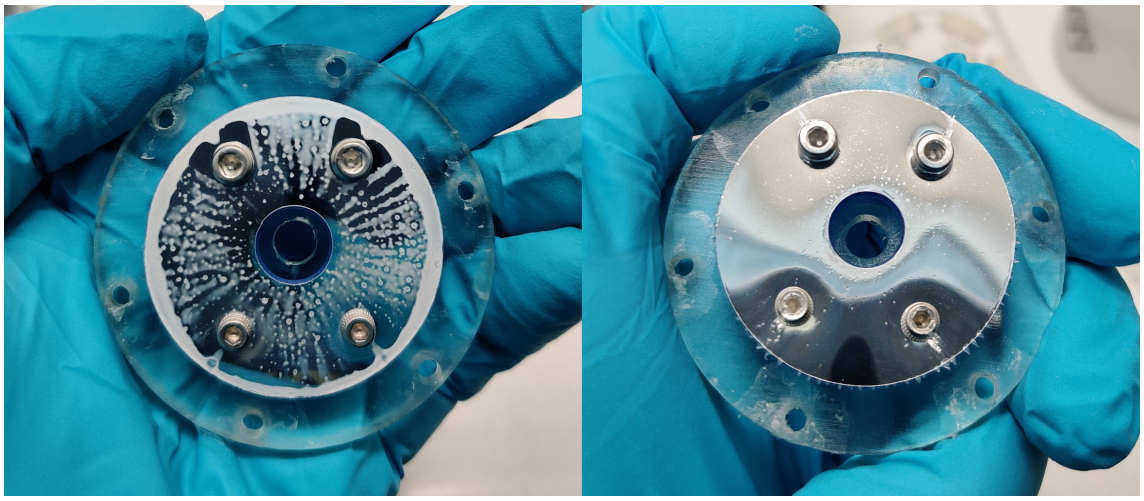

Figure 16: Two PET samples coated with PVDF-HFP. The left one is coated with 3 layers at 1300rpm, and the right one is coated with 10 layers at 2000rpm. The right one shows a much more even coating which can be visually evaluated.

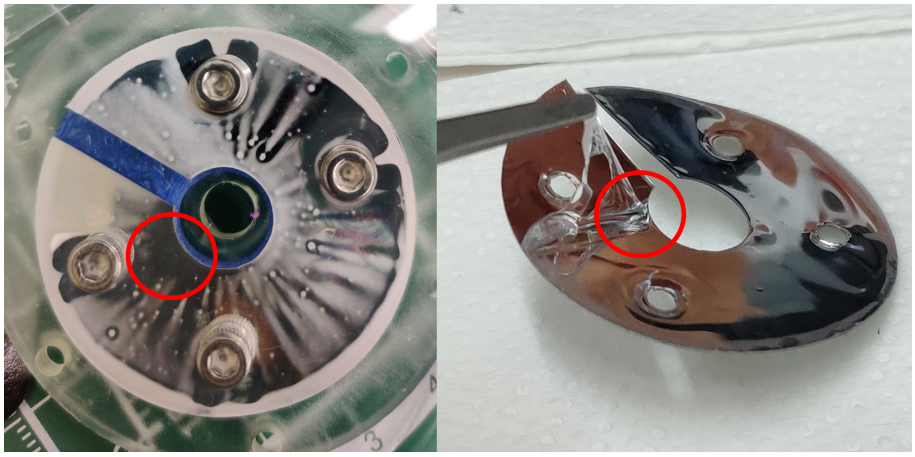

Figure 17: The first PET sample coated before and during peeling of the PVDF-HFP coating. Note the sections circled out in red, this indicates that a complete layer of PVDF-HFP covers the entire sample even at sections where the coating is almost invisible.

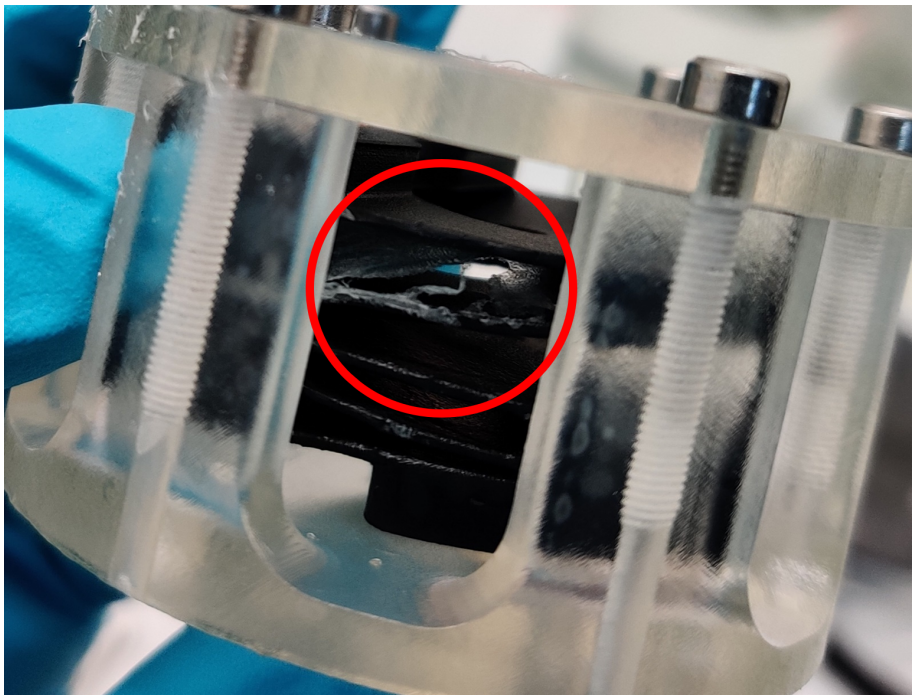

Figure 18: Helical electrode after multiple layers of PVDF-HFP coating. Note the coating layers sticking and separating circled out in red.

sample actuators made with PVDF-HFP coated electrodes showed premature breakdowns (As shown in Fig. 19) at as low as 500V during testing. This was believed to be caused by the thin coating thickness and low breakdown strength of PVDF-HFP. A potential fix was possible through the selection of better-fitting insulation polymers and solvent combinations. This was unfortunately not further explored due to time and resource limitations. The aforementioned success in Kapton insulation was used to fabricate the actuators for future experiments.

3 Experimental Results

Throughout the project development, several experiments were carried out to verify certain designs and evaluate some materials for the proposed helical actuators. This section aims to provide details on the sample preparation process and experimental setup of such experiments. The results of each experiment are discussed and lessons learned from those results are summarized.

3.1 ESD Ribbon

Several actuators with conventional flat ribbon electrodes were constructed to verify the material combination of the proposed actuator. The flat ribbon electrodes were also used to study the effects of the printing orientation on the resulting printing quality. Flat-ribbon electrodes were printed in HighTemp, Durable, ESD, and Clear resin from FormLabs on an SLA 3D printer (Form3, FormLabs). The printed electrodes then went through standard post-processing that consisted of washing, curing, and support removal. All parameters of the post-process were aligned with standard guidelines provided by FormLabs.

The finished electrodes were first evaluated manually for their mechanical properties. The electrodes were bent and their abilities to elastically return to the initial position were evaluated. The HighTemp resin was the first to be eliminated as the material was brittle and cracked even with a slight bend. ESD and Clear resin shared similar mechanical properties and were able to elastically return to the initial position. The Durable material was soft and was plastically deformed with the bend, unable to return to its initial position. However, the Durable material was still kept for

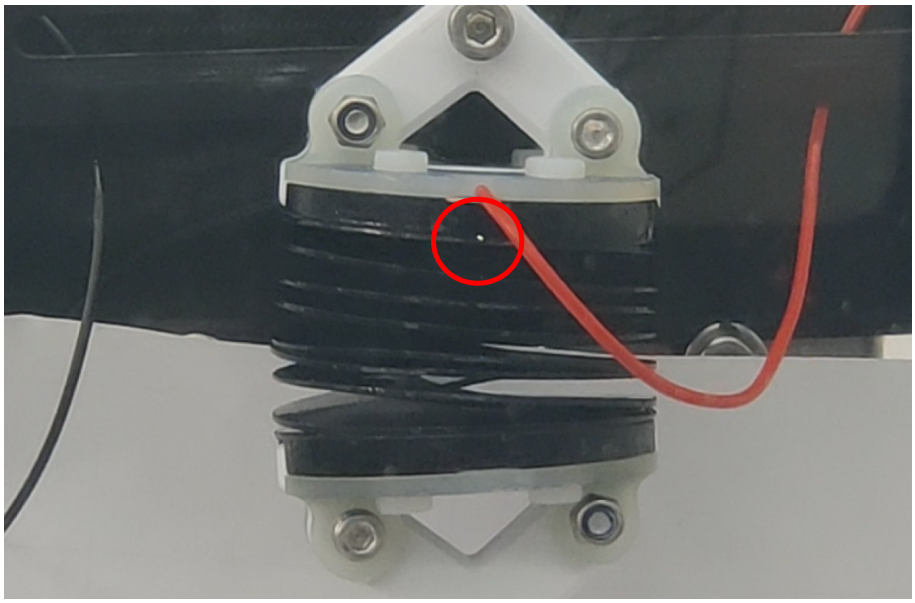

Figure 19: PVDF actuator when tested at 500V, note the breakdown arc circled out with red. This indicates a failure in the PVDF-HFP insulation layer.

the next tests thanks to its strength and ability to go through large deformations.

To evaluate the three remaining materials' mechanical properties for use in an actuator, pieces of copper tape were attached to the electrodes, and various insulation methods were used to insulate the copper tape. The electrodes were then assembled into actuators and tested with increasing voltages. For all tests, dielectric oil was injected in between the electrodes for improved dielectric performance and higher zipping force. All three materials showed zipping, but the actuators made with ESD and Clear showed zipping at a lower voltage than actuators made with Durable. This was believed to be the result of higher spring forces within the electrode structures. The durable material was thus also eliminated.

Apart from verifying the resin materials, the flat-ribbon tests also shed light on the feasibility of insulation methods. Three types of insulation were tested. The first insulation method was the application of PVC insulation tape. This was the same method that was used in the literature(Taghavi et al., 2018). Tests were successful and the actuator showed zipping when powered. However, the PVC tape wasn't able to adhere strongly to the printed electrodes. The thickness of the PVC tape, although not measured due to material softness, was also clearly thicker than the Kapton tape used later, making it inferior. The second insulation method tested was the wrapping of Mylar sheets. Mylar sheets were also used commonly in literature(Rothemund et al., 2021) and were proven to withstand up to 10kV. However, available Mylar sheets did not have adhesive and had to be wrapped around the electrodes manually and then fixed with another tape. This made it impossible to adapt this method to future helical electrodes. The insulation quality was also unstable and breakdowns happened already at 6kV. One potential explanation for this difference could be the folding and wrinkling involved in the wrapping process. Thirdly, Kapton tape with a thickness of 25um was applied and wrapped around the electrode for insulation. This method was proved best because the electrodes were able to show zipping and survived up to 10kV of driving voltage.

Finally, an additional test was done to examine the intrinsic conductivity of the ESD resin material. The ESD resin was infused with carbon and was claimed to be intrinsically conductive and ESD-safe. A pair of electrodes were printed with ESD resin and directly insulated with Kapton tape without the application of the copper tape. The resulting actuator showed zipping (shown in Fig. 20) and similar performance to the actuator made with copper tape. This made ESD superior to Clear resin as the intrinsic conductivity would play a key role in enabling the fabrication of the

helical electrodes.

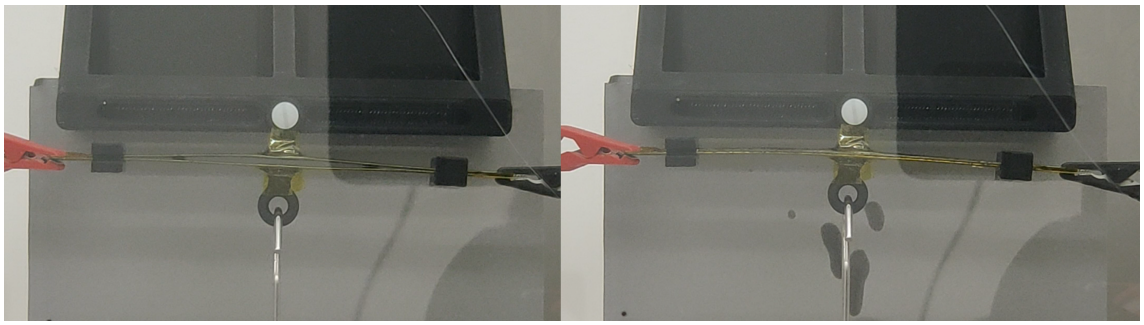

Figure 20: Testing ribbon actuator made with ESD, the left and right shows before and after application of 10kV across the electrodes. Zipping can be observed, the zipping is also very rapid and spills out the dielectric oil.

The ESD ribbon actuator experiments set the base of the helical actuators. The material combination of ESD resin as electrodes and Kapton as insulation was also verified to function. This material combination was then used for most actuators built for later tests.

3.2 Kapton Actuator V1

After iterations in design and printing orientation, a test actuator was made with helical electrodes. The helical electrodes were printed and post-processed. The post-processing of each electrode included removing the support structures, cleaning the inner surface by drilling the inner circle, carefully trimming and/or sanding away the outer surface imperfections, drilling and tapping all four mounting holes, and cleaning debris with pressurized air. Kapton tape was then carefully applied to one of the helical electrodes. Only one electrode was insulated to reduce the distance between electrodes when zipped with the hope of improving the actuator force. The application started by fixing the helical electrode to a fixture. Pieces of Kapton tape were then cut and carefully inserted sideways in between the helix to be attached to the bottom surface of the helix. After one piece of tape was attached, another piece was inserted and attached to the top surface aligning with the bottom piece of tape. The two pieces of tape were joined and trimmed to leave an overlap of around 10mm to ensure insulation. The failure to attach the tape usually required the previous piece of tape to be removed too. This was a very skill-intensive procedure and practice was needed before the failure rate was reduced. The insulation of a helical electrode with 10mm inner diameter, 50mm outer diameter, and 15 loops with 4mm pitch took around 6 hours and an estimated 200 pieces of Kapton tape.

After one of the helical electrodes was insulated, an actuator was assembled. Wires were first soldered to a piece of copper tape, which was then attached to one end of the electrodes. A small cut-out on the adaptor pieces on one end of the electrode was made to allow the wire to pass. This finished the fabrication of the actuator and it was ready to be tested. Steps in the fabrication process are shown in Fig. 21.

The finished actuator was attached to a fixture and connected to the High-Voltage Power Supply (HVPS) (Trek 20/20C, Maximum voltage 2kV). Dielectric oil (silicone oil M5) was injected in between the helix to improve dielectric performance. Breakdown happened when the HVPS was turned on starting at 2kV. Small arcs were visible at the far end of the electrodes as shown in Fig. 22. When the HVPS gave warning signals of output shorting, the HVPS was immediately shut down for protection. Those results indicated defects in the insulation of the electrodes. Further reflections of the experimental failure also suggested the reduction of helical loops for future electrode designs as discussed in 2.2.2. This would lead to shorter preparation times and less chance of failure thanks to the reduced length of the electrodes. Despite the failure, it was worth noting that the breakdown happened also at the far end of the electrode, this meant that electrical power was passed through the entire actuator and the conductivity of ESD resin wasn't

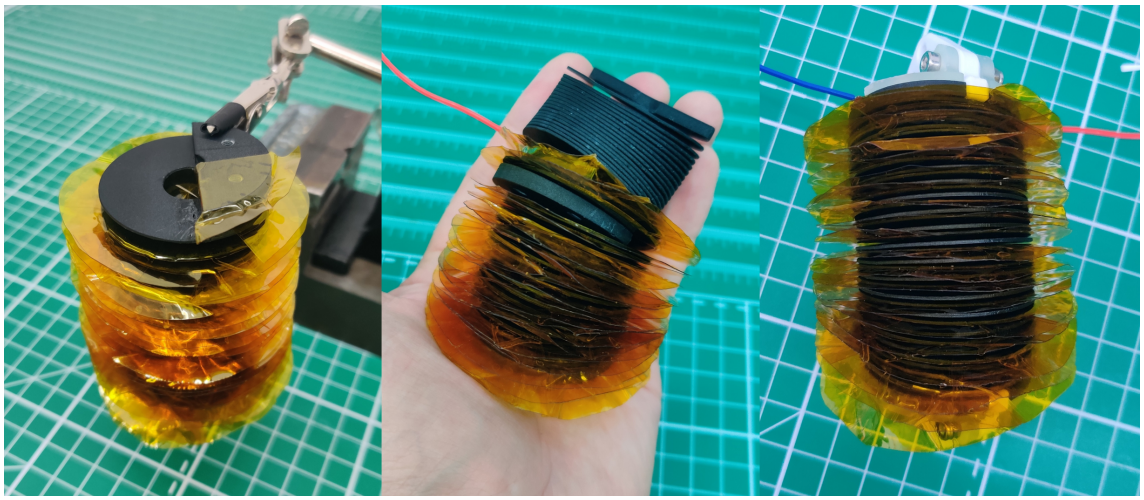

Figure 21: Fabrication of the Kapton Actuator. From left to right: insulating the electrode with Kapton, assembling two electrodes, and finishing the actuator.

a limiting factor. No more treatments would be necessary for the use of ESD resin for later helical actuator prototypes.

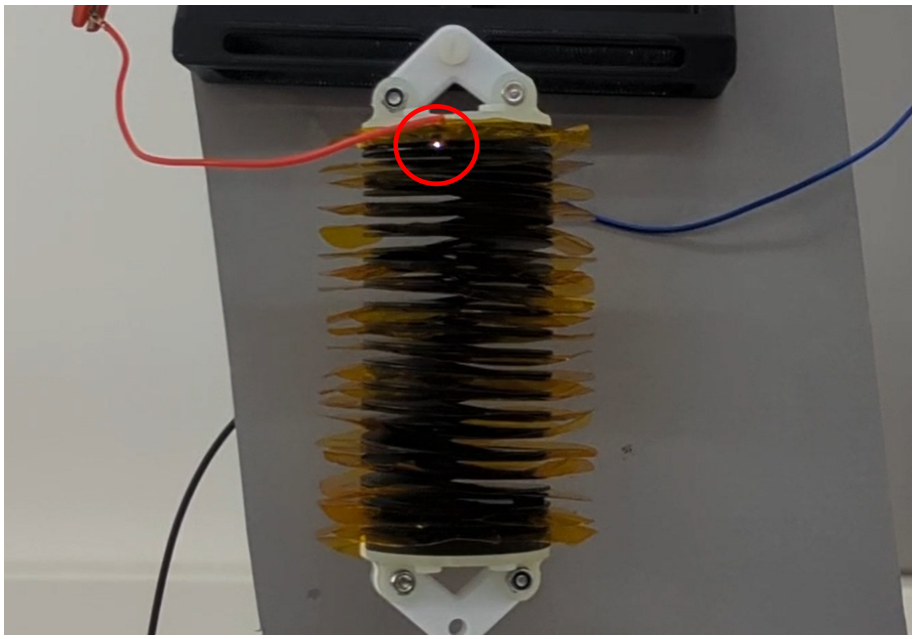

Figure 22: Testing the Kapton actuator V1 with 5kV. Note the breakdown arc circled out in red. This indicates defects in the insulation layer.

3.3 PVDF Actuator V1

After the failure of the Kapton-insulated helical electrodes, the alternative insulation method of PVDF-HFP coating was explored. Electrodes with reduced length (50mm outer diameter, 10mm inner diameter, 5 loops of 4mm pitch) were printed, post-processed, and prepared for insulation. Insulation was done by 1 layer of dip-spin-coating in a 15% weight solution of PVDF-HFP in Acetone solvent. This was due to issues with multi-layer coating discussed in 2.3.2. The helical electrode was dipped in the PVDF-HFP solution for 5 seconds, spun in the spinner machine for 300 seconds at 1200 rpm, and then left to dry for 300 seconds. This process was done on each of the two electrodes. The surface of the electrodes became glossy instead of the initial matte finish,

indicating successful coating. After insulation, the electrodes were assembled into an actuator, fixed to a fixture, and connected to a HVPS for testing. Dielectric oil (Silicone Oil M5) was injected in between the helix to improve the dielectric performance of the actuator.

Breakdown was already observed at 500V, a small arc was visible at the near end of the electrode as shown in Fig. 19. This indicated defects/failures in the insulation layer. The possible cause of this problem was believed to be surface roughness and thin coating thickness. The low electrical breakdown strength of PVDF-HFP could have also contributed to the premature breakdown. A potential fix to negate the insulation problem could be the replacement of the insulation material or an increase in the insulation layer thickness. However, further exploration was not carried out due to challenges discussed in 2.3.2. The technical pathway of PVDF-HFP coating was then put to the side for future studies. The conventional Kapton insulation was given higher priority since it was proven functional in previous flat-ribbon experiments.

3.4 Kapton Actuator V2

Following the findings from the first Kapton actuator experiment, design changes were made and an updated version of the actuator was developed. The updated electrode design featured an inner diameter of 70mm and an outer diameter of 120mm, and the helical loop count was further reduced to 3 while keeping the pitch at 2mm. The reduction of loop count was made to reduce the time needed to insulate the electrode since the circumference of the helix was larger due to the diameter increase. The mounting points connecting the electrode to the adaptor pieces were also increased from 2 to 4. This improved force distribution evenness on the adaptor piece and made the attachment of the electrodes to external loads more secure.

After printing and post-processing, one of the helical electrodes was insulated with Kapton tape. The application process was similar to that of the first helical actuator where pieces of Kapton tape were cut and applied in overlapping pairs. Thanks to extra space created by improved inner diameter, the Kapton tape could be joined in the middle and an overlap of 10mm was kept for both the inside and outside of the electrodes as shown in Fig. 23. The electrodes were then assembled into an actuator and connected to power with copper tapes.

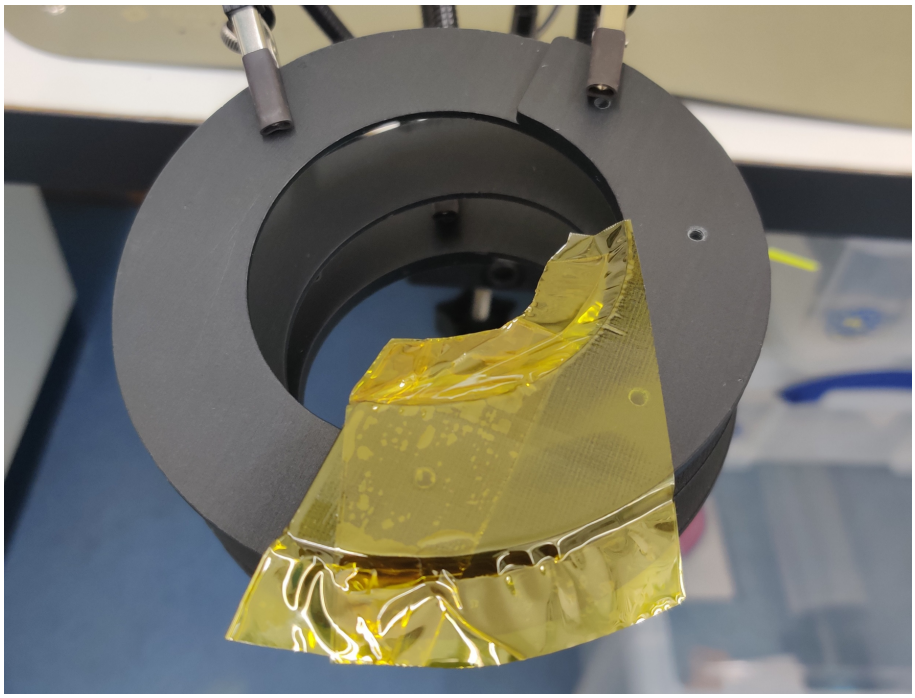

Figure 23: Taping Kapton actuator V2 with Kapton tape. Overlapping pairs of tape are applied along the electrode while maintaining a 10mm rim on both the inside and outside of the electrode.

Discussions were made within the lab regarding previous failures during testing. It was suggested that submerging the actuator in dielectric oil during testing might be beneficial for electrical breakdown protection. The oil had better dielectric properties than air and also had a higher breakdown strength. Following this suggestion, a small tank was filled with dielectric oil (EnviroTemp FR3). The finished actuator was suspended in the middle of the oil with a custom fixture. The actuator was observed to be very soft and the bottom side always dropped and rested on the bottom of the tank. The fixture was then made adjustable so that the initial height/length of the actuator could be adjusted. Reference pads with a 10mm grid were made from cutting pads and installed at the back and bottom sides of the tank to provide visual reference

The actuator started zipping at 3kV and was able to fully zip when powered with 5kV as shown in Fig. 24. The actuator stroke was observed from the front while taking reference with the grid pad in the back. The actuator was able to lift itself with a stroke of around 5-6mm. With a measured initial length of 17mm for the active section, this meant that the strain of the actuator was over 30%. The actuator force was estimated to be >1N. This was measured by holding the actuator at the same position on a scale and documenting the weight reading. This lifting force was purely generated from the electrostatic attraction between the electrodes since the helix structure was too soft and the spring forces were negligible. The actuator was also tested with increasing voltages and survived up to 8kV. The breakdown happened at 9kV and unfortunately damaged the actuator beyond repair. This stopped the actuator from being further evaluated.

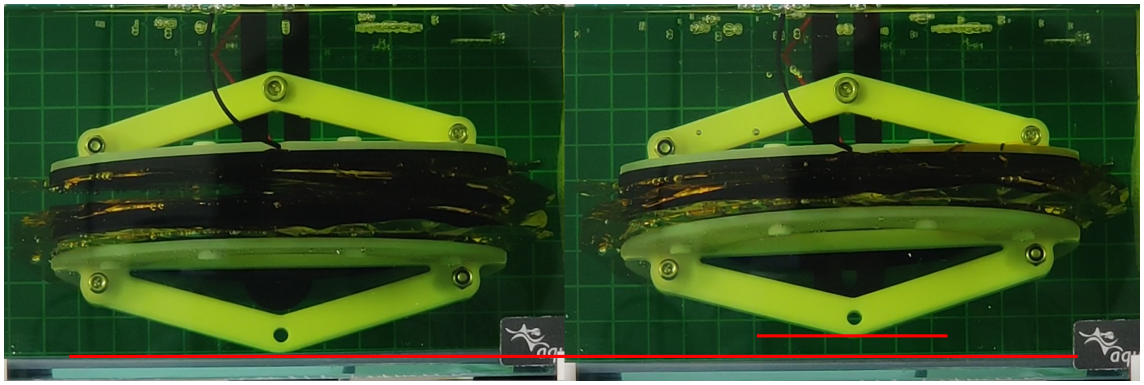

Figure 24: Testing the Kapton actuator V2 with 5kV. The left and right shows before and after the voltage was applied. Zipping can be observed and the contraction distance can be estimated to be around 5-6mm referencing the 10mm grid background.

This experiment served well as a proof of concept for the proposed helical actuator idea. The actuator was able to function as intended and survived a high voltage without breaking down. The Kapton insulation process was also verified to provide sufficient insulation for the electrodes for higher voltages. However, the electrode design had room for improvement. The V2 design still had the electrode thickness at 1mm. This thickness was too thin and did not provide a strong structure as shown in Fig. 25. This was not optimal for the actuator performance due to the lack of structural spring force during actuation. A thicker and stronger electrode was then designed for the next version.

3.5 Kapton Actuator V3

With lessons learned from previous experiments, a final version of the actuator was developed. The final actuator was mostly the same as the V2 design, except for thicker electrodes. The electrode thickness was increased to 3mm for a stronger structure and higher spring forces during actuation. All other fabrication processes were the same as those of Version 2. During the application of Kapton insulation, the helical electrode had to be bent to open up space for the tape to fit through. Since the Version 3 electrode design was thicker, stiffer, and harder to deform, the Kapton application process was noticeably more difficult. This suggested that the room for potential thickness increase would be limited. Much thicker electrodes would be impossible to open wide

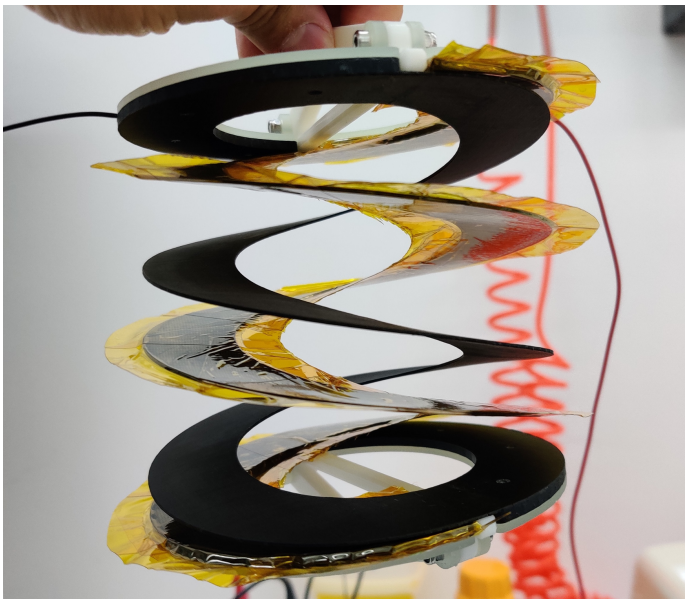

Figure 25: Holding the Kapton actuator V2. The actuator opens much wider than initially designed. This is due to the helical electrode being too soft and unable to support the weight of the actuator.

enough to apply Kapton tape and cannot be made into actuators with the current fabrication process.

Version 3 was tested in air since actuation in oil was already verified and there wasn't enough time to conduct more experiments in oil. A custom experimental setup was constructed to test the final version 3 actuator in air. An adjustable bottom support was designed and allowed the initial actuator length to be varied. An adjustable weight was connected to the bottom of the actuator and the weight position/height was monitored by a laser distance sensor (Baumer 0m70). The testing setup is shown in Fig. 26. This setup was built to measure the force and strain of the actuator simultaneously. The actuator again showed movement and some zipping at 3kV, but unfortunately broke down at around 5kV. Electrical arcing and smoke could be observed, and a small section of the electrode was burnt away (As shown in Fig. 27). Attempts were made to repair and reinforce the Kapton insulation by adding patches of Kapton tape. However, more breakdowns happened and damaged the actuator further.

Although time and resources did not allow further repairs and tests to be done, the test was partially successful as the actuator showed similar zipping movement in air when compared with in-oil experiments. The premature breakdown was most likely caused by reduced breakdown protection from the reduced dielectric oil between the electrodes. This could potentially be solved by an oil-filled enclosure wrapping around the actuator. This enclosure would allow more dielectric oil to be trapped between the electrodes for protection. If time and resources allowed, an updated version resolving the breakdown issue would be possible to function in the air and integrated into robotic applications.

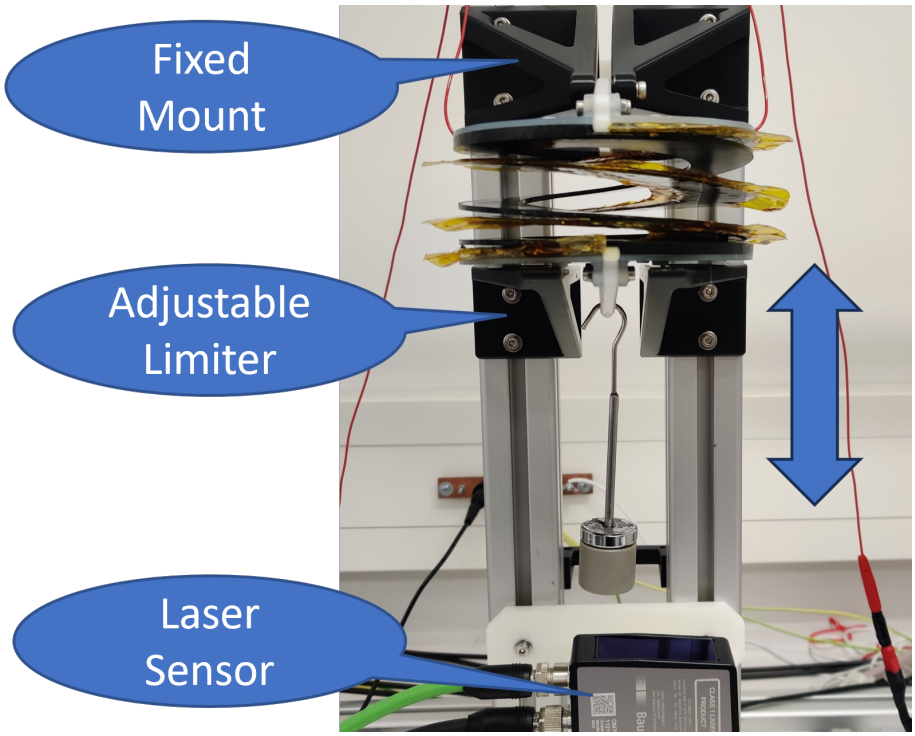

Figure 26: Experiment setup for Kapton actuator V3. The actuator is mounted to a fixed mount and the bottom is supported by an adjustable limiter. The position of the weight attached to the actuator is monitored with a laser sensor.

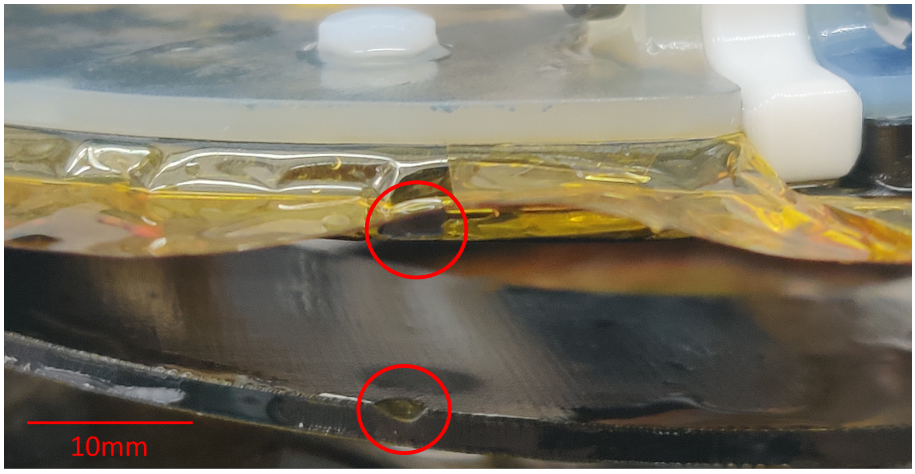

Figure 27: Close-up picture of Kapton actuator V3 after breakdown. Note the burnt-away Kapton tape and the corresponding burnt section on the other electrode circled out in red.

4 Discussions

This section provides discussions on the experimental results and experiences obtained during the development of the thesis project. Pathways that can potentially lead to better actuator performance are also discussed.

4.1 Improving Actuator Force

The actuator force observed during the experiments is not satisfactory for the actuator to be used in a robotic setting. The initial goal of the project targets actuators with a form factor similar to the human bicep muscle (approximated 50mm diameter, 90mm height pillar shape), but even actuator designs with a much larger size (120mm outer and 70mm inner diameter) are only able to generate 1N of pulling force. It will be thus beneficial to discuss factors that can contribute to actuator force improvements and provide guidelines for potential future improvements.

Discussions on force generation can be simplified by considering the flat ribbon actuators that inspired this project. This is because the proposed double helical actuators share the same actuation principle, and the innovation lies mainly in the structural improvements that allow more compact actuators with efficient stacking. The total force can also be improved as the helical structure will allow each electrode to be shared by two principal actuators.

The actuation force of an electro-ribbon actuator comes from two sources: the restorative elastic spring force of the electrode structure, and the electrostatic attraction forces between the electrodes. The total actuator force will be the combination of the above two forces. The spring force is proportional to the stiffness of the electrode material, the thickness of the electrode, and the amount of deformation of the electrode. Across the actuation/zipping process of the actuator, the spring force decreases as the electrode returns to its initial/default shape. The spring force can thus be improved by using stiffer materials, such as metals, to construct the electrodes. The thickness of the electrode can also be increased to improve the overall stiffness of the electrodes. The electro-ribbon actuator that generated the highest force is constructed with the thickest metal strips, this agrees with the above theory.

The electrostatic force in flat ribbon actuators having parallel electrodes can be expressed as in Equation (1)(Taghavi et al., 2018). In the equation, $\varepsilon_{r-medium}$ and t_{medium} represent the relative permittivity and thickness of the liquid medium (Silicon Oil), $\varepsilon_{insulator}$ and $t_{insulator}$represents the relative permittivity and thickness of the insulator, ε_0 represents the vacuum permittivity, A represents the electrode area, and V represents the driving voltage across the electrodes.

The electrostatic force is inversely proportional to the square of the distance between the electrodes and increases as the electrodes move closer during actuation. This means that a thinner insulation layer will allow the electrodes to be pulled closer when zipped and generate higher electrostatic forces. The electrostatic force is also proportional to the total dielectric permittivity of the insulation material as well as the medium between two electrodes during actuation. This means that changing into materials, such as P(VDF-TrFE-CTFE) Terpolymer, with higher dielectric permittivity will improve the electrostatic force. Similar improvements can also be achieved by replacing air between electrodes with dielectric oils having a higher permittivity, such as EnviroTemp FR3 and Silicone oil. Thirdly, the electrostatic force is proportional to the square of the driving voltage across the electrodes. This means that a higher driving voltage can significantly improve the electrostatic zipping force of the actuator if insulated successfully. A thorough analysis of electrostatic force optimizations was summarized in Hinchet and Shea (2020). As discussed in the above literature, the electrostatic force can be optimized by maximizing the insulator figure of merit. This is defined as $\varepsilon_{r-medium}E_{breakdown}$, where $E_{breakdown}$ is the breakdown electric field of the insulator. Finally, the zipping force is also proportional to the electrode areas, this means that making the electrodes longer and wider can improve the maximum force of the actuator. With the helical concept discussed in this thesis, this translates into helical electrodes with larger outer diameter, smaller inner diameter, and denser packaging (lower pitch).

$$F_{attraction} = \frac{1}{2} \frac{\varepsilon_{r-medium} \varepsilon_0 A V^2}{\left(\frac{\varepsilon_{r-medium}}{\varepsilon_{insulator}} t_{insulator} + t_{medium} \right)^2} \tag{1}$$

With the above analysis, the ideal actuator that focuses on maximizing force output can be potentially constructed with metal electrodes with optimal thickness. The electrodes are insulated from a high driving voltage with thin layers of high dielectric permittivity material. The figure of merit of the insulation, defined by $\varepsilon_{r-medium} E_{breakdown}$, should also be optimized. The actuator packaging should contain dielectric oil with high dielectric permittivity and the actuator electrode dimensions should be maximized.

4.2 Choice of Driving Voltage

Another important topic for future researchers will be the choice of driving voltage. Here we distinguish high voltages from low voltages by mean of under or above 1kV. 1kV is where significant differences in component supply and safety regulations can be observed. High voltage (HV) components (Power supplies, amplifiers, switches) are larger and also less accessible due to limited supply and higher cost. Machines running with high voltage also have to go through much stricter safety regulations. On the other hand, low voltage (LV) electronics are more available and the form factor can also be reduced (Mitchell et al., 2022). Each choice will lead to different technical pathways as well as application scenarios. The major design difference between HV and LV designs is the insulation process.

HV designs require insulation materials with a higher electrical breakdown strength such as Kapton (Polymide). The insulation layer can also be thicker to prevent electrical breakdowns, which is more dangerous when high voltages are involved, depending on the electronic maximum power. High voltage leads to higher current when breakdowns happen and the risk of ignition will be higher with excess heat from the high current. Since HV components are usually bulky and not portable, the actuator design driven by HV will be a better fit for stationary applications in a structured environment, such as on a factory floor. In those application scenarios, mobility of the actuator will not be a concern and the risk of electrical shock can be minimized by carefully managing human-robot interactions. One example application can be robot arms powered by HV actuators to serve pick-and-place tasks in factories.

LV designs can be enabled by the use of insulating materials with higher dielectric permittivity such as PVDF-HFP. Such materials can have 3 times the dielectric performance of Kapton, but unfortunately also have lower breakdown strength and cannot survive high electric fields. When a low voltage is used as driving voltage, the electronics used for the actuator can be much smaller and portable. A lower voltage also reduces the risk of electrical shocks and fire hazards during breakdowns. Those features mean that LV designs will be a better fit for mobile applications and able to serve closer interactions with the environment as well as humans. One example application can be robot dogs powered by LV actuators and serve the task of human companionship.

4.3 Potentials

The actuator fabrication and verification experiments didn't go smoothly and only a few quantitative data were gathered. However, it is possible to discuss the potential of the actuator and to evaluate whether the initial target performance will be achievable with the current progress.

The Kapton actuator V2 was tested in oil and was able to generate around 1.2N of electrostatic pulling force and a strain of around 30% when powered with 5kV. Since the insulation of the actuator was verified to survive 8kV, the maximum electrostatic force can be scaled up by the square of 8kV/5kV up to 3.072N. The spring force contribution in the V2 design was negligible. However, an actuator constructed later with thicker electrodes should at least be able to support its weight with its spring forces. This means that there will be a spring force component of >1.2N in the total pulling force. The total expected pulling force can then be added up to >4.2N. This means that a force of at least 4.2N can be achieved with the existing fabrication process. The

insulation material (Kapton) was verified to be capable of surviving voltages up to 10kV in the flat ribbon experiments (discussed in 3.1). Therefore the possibility of constructing an actuator capable of 10kV driving voltage with the current fabrication process will be very high. Such an actuator will then have an electrostatic force of 4.8N and a total force of >6N.

Since the initial goal for the actuator performance is set to be 5N of pulling force at 30% strain, the possibility of achieving this goal with the current project progress will be very high. The only limitation is the time and resource constraints that hinder the fabrication and testing of more actuator samples with more experimental settings.

5 Future Work

This section aims to provide some ideas for future work on improving and further developing the proposed double-helical electrostatic actuators.

5.1 Modeling and Simulations

Actuator modeling and simulations were planned to be carried out after initial verification of the actuator concept. However, this was not possible due to repeated failures with electrode insulation and limitations on time and resources. In future studies, an analytical model of the actuator can be constructed. Such a model should take in the material properties of the electrode material, driving voltage, and current actuator state to calculate the pulling force of the actuator. Knowledge of solid mechanics and electrostatics will be crucial in constructing such a model. The accuracy of the model can be verified when compared with experimental data. Once the physical model can accurately predict the actuator performance, simulations in multi-physics simulators such as COMSOL Multiphysics can be set up to simulate the performance of new actuator designs. Design optimizations can then be carried out in simulation to be faster and more efficiently iterated. Electrode materials can be selected without physical construction and dimensional changes can also be evaluated. With optimized material choice and structural design, the double helix actuator performance has the potential to be improved much further.

5.2 In-Oil Experiments

Dielectric oil protects the actuator from breakdowns compared to air and can improve the performance of the actuator. This was verified by testing Kapton actuator V2 submerged in EnviroTemp FR3 oil. However, the experiment wasn't able to fully test the potential performance of the actuator due to premature breakdown at 9kV damaging the actuator electrodes. Accurate quantitative measurements were also not possible due to time limitations.

More quantitative experiments with the actuator submerged in oil will potentially lead to more quantitative data. The actuator can be fixed to the bottom of the oil tank and connected to an external weight with a pulley system. The position/height of the weight can be measured by an external distance sensor such as a laser displacement sensor. This setup will allow measurement of the actuator strain at various loads. Another option will be to connect the actuator to a force gauge with the pulley system and adjust the position of the force gauge with a linear motion setup. This will allow measurement of the actuator force at adjustable strain locations.

More experiments in oil will also enable researchers to verify the maximum performance of the actuators. With increased driving voltage up to 8kV, the electrostatic force of the actuator can be improved by 2.5 times. It will also be interesting to test the possibility of encapsulating dielectric oil around the actuator with a flexible outer skin. Such encapsulation can greatly improve the mobility of the actuator if successful.

5.3 Dip-Coating of PVDF-HFP

The ability to insulate the electrodes with PVDF-HFP has a great potential to improve the performance of the actuator. This is because PVDF-HFP has a dielectric permittivity of 10 compared

with Kapton which has 3. This means that the electrostatic force can be >3 times higher with PVDF-HFP at the same applied voltage. P(VDF-TrFE-CTFE) Terpolymer further increases the permittivity to 47, around 16 times force improvements compared with Kapton for the same applied voltage. The main reason for the insulation layers failing with PVDF actuator V1 experiments could have been that the thickness was too thin and the roughness too high in comparison. This means that the breakdown issue can potentially be solved with thicker PVDF-HFP coatings. There are two ways to achieve thicker coatings. Firstly, the PVDF-HFP solution used was with a weight concentration of 15%, the concentration can be increased to increase the viscosity of the solution. A more viscous solution will better cover the electrodes and more PVDF-HFP can be deposited to form thicker layers. The other way to improve coating thickness will be to reduce or remove the spinning process. This is because the spinning process removes the excess solution as well as spreads it and the reduced amount of coating solution remaining leads to thinner coating layers. A dip-coating holder without spinning, as shown in Fig. 28, was constructed but unfortunately not tested due to time limitations.

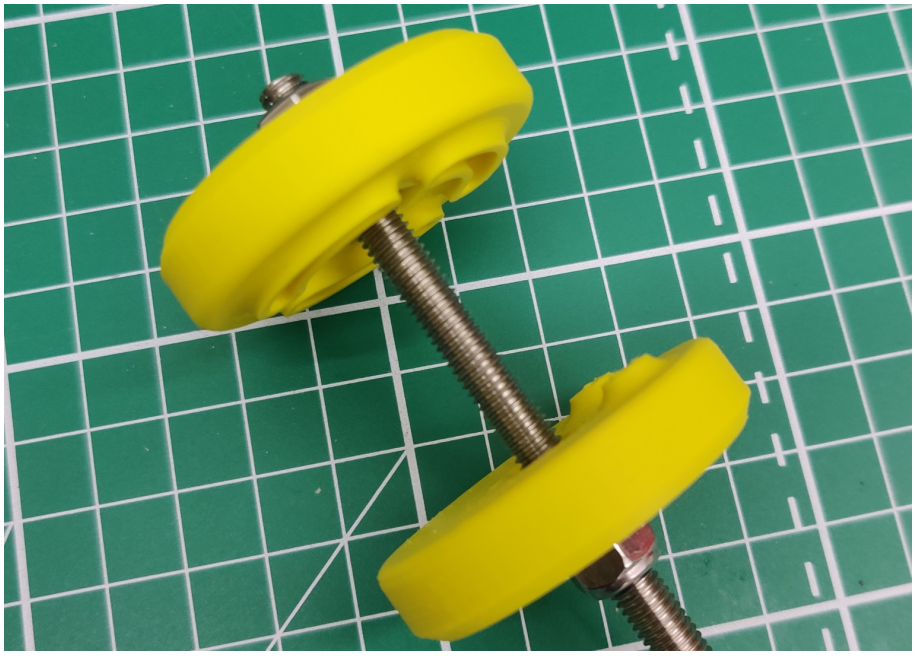

Figure 28: An adjustable dipping holder prepared for the dip-coating of PVDF-HFP for the electrodes. The helical electrode can be held at variable stretch positions when installed. The induced twist of the electrode can be compensated by the slotted holder on the top side of the figure.

Combining the two adjustments mentioned above with the PVDF-HFP coating process can potentially lead to much thicker PVDF-HFP insulation for the electrodes. The resulting electrodes can then be assembled into actuators and tested with lower voltages below 1kV. If functional, the performance of the LV actuators can be compared with the HV actuators. Portable driving and control electronics can then also be developed to enable future integration experiments of the LV actuators.

5.4 DHESA v.s. HASEL

The HASEL actuators represent the latest developments in electrostatic actuator technology. It will be beneficial in the future to compare DHESA actuators with HASEL actuators regarding key performance metrics such as power density, stress-strain relationship, efficiency, and durability. The discussions and analysis following such comparisons can be of great value for the future development of artificial muscles.

6 Acknowledgements

The author would like to acknowledge the contributions and assistance given by fellow researchers throughout the project development. Their kind help and guidance were crucial in moving the project forward and were greatly appreciated.

Thanks to Prof. Robert Katzschmann for supporting the project ideas, providing essential resources for experiments, and helpful guidance on high-level planning of the project.

Thanks to Mr. Amirhossein Kazemipour for supervising the project, hosting weekly meetings for suggestions, and coordinating the project execution.

Thanks to Dr. Ronan Hinchet for constructive guidance and inspiration regarding fabrication, electrostatic physics, and material science. The suggestions and assistance given were very useful as the author didn't have prior experience with underlying material science for electrostatic actuators.

Thanks to Mr. Stephan-Daniel Gravert and Mr. Elias Varini for their suggestions and knowledge regarding actuator fabrication and testing. Such knowledge enabled the successful testing of the double-helical actuator.

Thanks to Mr. Thomas Buchner for managing equipment and resources around the laboratory. The project would suffer much more hardship without the efficient and structured infrastructure created by his work.

References

Acome, E., Mitchell, S. K., Morrissey, T. G., Emmett, M. B., Benjamin, C., King, M., Radakovitz, M., & Keplinger, C. (2018). Hydraulically amplified self-healing electrostatic actuators with muscle-like performance [Publisher: American Association for the Advancement of Science]. *Science*, *359*(6371), 61–65. https://doi.org/10.1126/science.aao6139 (cit. on p. 1)

Carpi, F., Migliore, A., Serra, G., & Rossi, D. D. (2005). Helical dielectric elastomer actuators. *Smart Materials and Structures*, *14*(6), 1210. https://doi.org/10.1088/0964-1726/14/6/014 (cit. on p. 2)

Della Schiava, N., Pedroli, F., Thetpraphi, K., Flocchini, A., Le, M.-Q., Lermusiaux, P., Capsal, J.-F., & Cottinet, P.-J. (2020). Effect of beta-based sterilization on P(VDF-TrFE-CFE) terpolymer for medical applications [Number: 1 Publisher: Nature Publishing Group]. *Scientific Reports*, *10*(1), 8805. https://doi.org/10.1038/s41598-020-65893-2 (cit. on p. 14)

Garrad, M., Zadeh, M. N., Romero, C., Scarpa, F., Conn, A. T., & Rossiter, J. (2022). Design and Characterisation of a Muscle-Mimetic Dielectrophoretic Ratcheting Actuator [Conference Name: IEEE Robotics and Automation Letters]. *IEEE Robotics and Automation Letters*, *7*(2), 3938–3944. https://doi.org/10.1109/LRA.2022.3149039 (cit. on p. 1)

Hawkes, E. W., Majidi, C., & Tolley, M. T. (2021). Hard questions for soft robotics [Publisher: American Association for the Advancement of Science]. *Science Robotics*, *6*(53), eabg6049. https://doi.org/10.1126/scirobotics.abg6049 (cit. on p. 1)

Helps, T., Romero, C., Taghavi, M., Conn, A. T., & Rossiter, J. (2022). Liquid-amplified zipping actuators for micro-air vehicles with transmission-free flapping [Publisher: American Association for the Advancement of Science]. *Science Robotics*, *7*(63), eabi8189. https://doi.org/10.1126/scirobotics.abi8189 (cit. on p. 1)

Hinchet, R., & Shea, H. (2020). High Force Density Textile Electrostatic Clutch [_eprint: https://onlinelibrary.wiley.com *Advanced Materials Technologies*, *5*(4), 1900895. https://doi.org/10.1002/admt.201900895 (cit. on p. 27)

Hutter, M., Gehring, C., Jud, D., Lauber, A., Bellicoso, C. D., Tsounis, V., Hwangbo, J., Bodie, K., Fankhauser, P., Bloesch, M., Diethelm, R., Bachmann, S., Melzer, A., & Hoepflinger, M. (2016). ANYmal - a highly mobile and dynamic quadrupedal robot [ISSN: 2153-0866]. *2016 IEEE/RSJ International Conference on Intelligent Robots and Systems (IROS)*, 38–44. https://doi.org/10.1109/IROS.2016.7758092 (cit. on p. 1)

Katzschmann, R. K., DelPreto, J., MacCurdy, R., & Rus, D. (2018). Exploration of underwater life with an acoustically controlled soft robotic fish [Publisher: Science Robotics Section: Research Article]. *Science Robotics*, *3*(16). https://doi.org/10.1126/scirobotics.aar3449 (cit. on p. 1)

Kellaris, N., Gopaluni Venkata, V., Smith, G. M., Mitchell, S. K., & Keplinger, C. (2018). Peano-HASEL actuators: Muscle-mimetic, electrohydraulic transducers that linearly contract on activation [Publisher: American Association for the Advancement of Science]. *Science Robotics*, *3*(14), eaar3276. https://doi.org/10.1126/scirobotics.aar3276 (cit. on pp. 2, 14)

Kellaris, N., Rothemund, P., Zeng, Y., Mitchell, S. K., Smith, G. M., Jayaram, K., & Keplinger, C. (2021). Spider-Inspired Electrohydraulic Actuators for Fast, Soft-Actuated Joints [_eprint: https://onlinelibrary.wiley.com/doi/pdf/10.1002/advs.202100916]. *Advanced Science*, *8*(14), 2100916. https://doi.org/10.1002/advs.202100916 (cit. on p. 1)

Kellaris, N., Venkata, V. G., Rothemund, P., & Keplinger, C. (2019). An analytical model for the design of Peano-HASEL actuators with drastically improved performance. *Extreme Mechanics Letters*, *29*, 100449. https://doi.org/10.1016/j.eml.2019.100449 (cit. on p. 2)

Laschi, C., Mazzolai, B., & Cianchetti, M. (2016). Soft robotics: Technologies and systems pushing the boundaries of robot abilities [Publisher: American Association for the Advancement of Science]. *Science Robotics*, *1*(1), eaah3690. https://doi.org/10.1126/scirobotics.aah3690 (cit. on p. 1)

Li, G., Chen, X., Zhou, F., Liang, Y., Xiao, Y., Cao, X., Zhang, Z., Zhang, M., Wu, B., Yin, S., Xu, Y., Fan, H., Chen, Z., Song, W., Yang, W., Pan, B., Hou, J., Zou, W., He, S., … Yang, W. (2021). Self-powered soft robot in the Mariana Trench [Number: 7848 Publisher:

Nature Publishing Group]. *Nature*, *591*(7848), 66–71. https://doi.org/10.1038/s41586-020-03153-z (cit. on p. 1)

Marchese, A. D., Katzschmann, R. K., & Rus, D. (2015). A Recipe for Soft Fluidic Elastomer Robots [Publisher: Mary Ann Liebert, Inc., publishers]. *Soft Robotics*, *2*(1), 7–25. https://doi.org/10.1089/soro.2014.0022 (cit. on p. 1)

Mitchell, S. K., Martin, T., & Keplinger, C. (2022). A Pocket-Sized Ten-Channel High Voltage Power Supply for Soft Electrostatic Actuators [_eprint: https://onlinelibrary.wiley.com/doi/pdf/10.1002/admt. *Advanced Materials Technologies*, *7*(8), 2101469. https://doi.org/10.1002/admt.202101469 (cit. on p. 28)

Nishimura, S., Masuyama, S., Shimizu, G., Chen, C.-Y., Ichibayashi, T., & Watanabe, J. (2022). Lowering of Electrostatic Actuator Driving Voltage and Increasing Generated Force Using Spontaneous Polarization of Ferroelectric Nematic Liquid Crystals [_eprint: https://onlinelibrary.wiley.com/doi *Advanced Physics Research*, *1*(1), 2200017. https://doi.org/10.1002/apxr.202200017 (cit. on pp. 2, 5)

O'Halloran, A., O'Malley, F., & McHugh, P. (2008). A review on dielectric elastomer actuators, technology, applications, and challenges [Publisher: American Institute of Physics]. *Journal of Applied Physics*, *104*(7), 071101. https://doi.org/10.1063/1.2981642 (cit. on pp. 1, 14)

Rothemund, P., Kellaris, N., Mitchell, S. K., Acome, E., & Keplinger, C. (2021). HASEL Artificial Muscles for a New Generation of Lifelike Robots—Recent Progress and Future Opportunities [_eprint: https://onlinelibrary.wiley.com/doi/pdf/10.1002/adma.202003375]. *Advanced Materials*, *33*(19), 2003375. https://doi.org/10.1002/adma.202003375 (cit. on p. 20)

Rothemund, P., Kirkman, S., & Keplinger, C. (2020). Dynamics of electrohydraulic soft actuators. *Proceedings of the National Academy of Sciences*, *117*(28), 16207–16213. https://doi.org/10.1073/pnas.2006596117 (cit. on p. 2)

Sîrbu, I. D., Moretti, G., Bortolotti, G., Bolignari, M., Diré, S., Fambri, L., Vertechy, R., & Fontana, M. (2021). Electrostatic bellow muscle actuators and energy harvesters that stack up [Publisher: American Association for the Advancement of Science]. *Science Robotics*, *6*(51), eaaz5796. https://doi.org/10.1126/scirobotics.aaz5796 (cit. on p. 1)

Taghavi, M., Helps, T., & Rossiter, J. (2018). Electro-ribbon actuators and electro-origami robots [Publisher: American Association for the Advancement of Science]. *Science Robotics*, *3*(25), eaau9795. https://doi.org/10.1126/scirobotics.aau9795 (cit. on pp. 2, 3, 20, 27)

Wang, X., Mitchell, S. K., Rumley, E. H., Rothemund, P., & Keplinger, C. (2020). High-Strain Peano-HASEL Actuators [_eprint: https://onlinelibrary.wiley.com/doi/pdf/10.1002/adfm.201908821]. *Advanced Functional Materials*, *30*(7), 1908821. https://doi.org/10.1002/adfm.201908821 (cit. on p. 1)

Yasa, O., Toshimitsu, Y., Michelis, M. Y., Jones, L. S., Filippi, M., Buchner, T., & Katzschmann, R. K. (2023). An Overview of Soft Robotics [_eprint: https://doi.org/10.1146/annurev-control-062322-100607]. *Annual Review of Control, Robotics, and Autonomous Systems*, *6*(1), 1–29. https://doi.org/10.1146/annurev-control-062322-100607 (cit. on p. 1)

Zhu, J., White, C., Wainwright, D. K., Santo, V. D., Lauder, G. V., & Bart-Smith, H. (2019). Tuna robotics: A high-frequency experimental platform exploring the performance space of swimming fishes [Publisher: Science Robotics Section: Research Article]. *Science Robotics*, *4*(34). https://doi.org/10.1126/scirobotics.aax4615 (cit. on p. 1)

Eidgenössische Technische Hochschule Zürich
Swiss Federal Institute of Technology Zurich

Title of work:

Electrostatic Zipping Actuators With A Double-Helical Structure

Thesis type:

Master's Thesis Report

Student:

Name:	Yu (Antares) Zhang
E-mail:	zhangyu@ethz.ch
Student ID:	18-913-277

Supervisors:

Dr. Ronan Hinchet
Prof. Dr. Robert Katzschmann

Declaration of originality

I hereby confirm that I am the sole author of the written work here enclosed and that I have compiled it in my own words. Parts excepted are corrections of form and content by the supervisor.

With my signature I confirm that

- I have committed none of the forms of plagiarism described in the 'Citation etiquette' information sheet.
- I have documented all methods, data and processes truthfully.
- I have not manipulated any data.
- I have mentioned all persons who were significant facilitators of the work.

I am aware that the work may be screened electronically for plagiarism.

Signature: Zürich, November 12, 2023 _____